DV1.3 Accounting for Stress History and Lithology through Forward Geomechanical Modelling

Organisation(s)	Rockfield
Author(s)	Dan Roberts, Dan Phillips
Reviewer	Jung Chan Choi, Lars Grande
Type of deliverable	Report
Dissemination level	Public
WP	1.3
Issue date	September 2023
Document version	1

Keywords: Stress, diagenesis, pore pressure, geomechanical modelling, yield surface, critical state soil mechanics, finite element method.

Summary:
A core theme of the SHARP project is integrating the stress history of the North Sea basins into stress characterisation and experimental testing procedures, and by extension developing an appreciation for how this might influence assessment of risk and monitoring requirements for storage operations. The link here is geomechanical modelling, which facilitates predictions of subsurface deformation as a function of evolving stress conditions and the experimentally constrained constitutive properties. This report documents a suite of geomechanical models applied to the Horda platform area of northern North Sea. Evolutionary models of the Troll area are presented, with specific focus on well 31/6-1, which examine the significance of burial history, chemical compaction and uplift/glaciation on stress and pore pressure in the area. When explicitly representing these processes and leveraging understanding of mineralogical significance developed in earlier tasks it is found that these support log-based workflows presented in Deliverable 1.2. Conclusions regarding the probable causes for elevated shallow stresses and pore pressures at these sites are made. Preliminary efforts to direct the procedures and techniques to the Smeaheia alpha well 32/4-1 are shown.

The key findings of the modelling work are summarised and implications for risk and monitoring are presented. Concepts for extending the work within 3D geomechanical models are provided and will be tackled in subsequent project tasks.

Contents

1 Introduction

1.1 Overview

This report aims to assess methods and procedures for incorporating stress history into geomechanical models. Models adopt an evolutionary forward modelling process that explicitly represents the key geological processes which can include mechanical and chemical compaction, uplift and glaciation. Lithological significance is an important component of the work and expands upon constitutive modelling work developed during SHARP Work Package 1.2.

1.2 Geological Setting for Study Area – Horda Platform, Northern North Sea

The focus area for investigations is the eastern area of Northern North Sea (Figure 1-1). The primary Area of Interest (AOI) is the Horda Platform, and primarily the Troll East field (block 31/6) and the Smeaheia area (blocks 32/2 and 32/4). This area has been selected as it is targeted for storage operations within the SHARP project and has been the subject of *in situ* stress investigation in preceding work packages (SHARP WP1.2 Report, 2023).

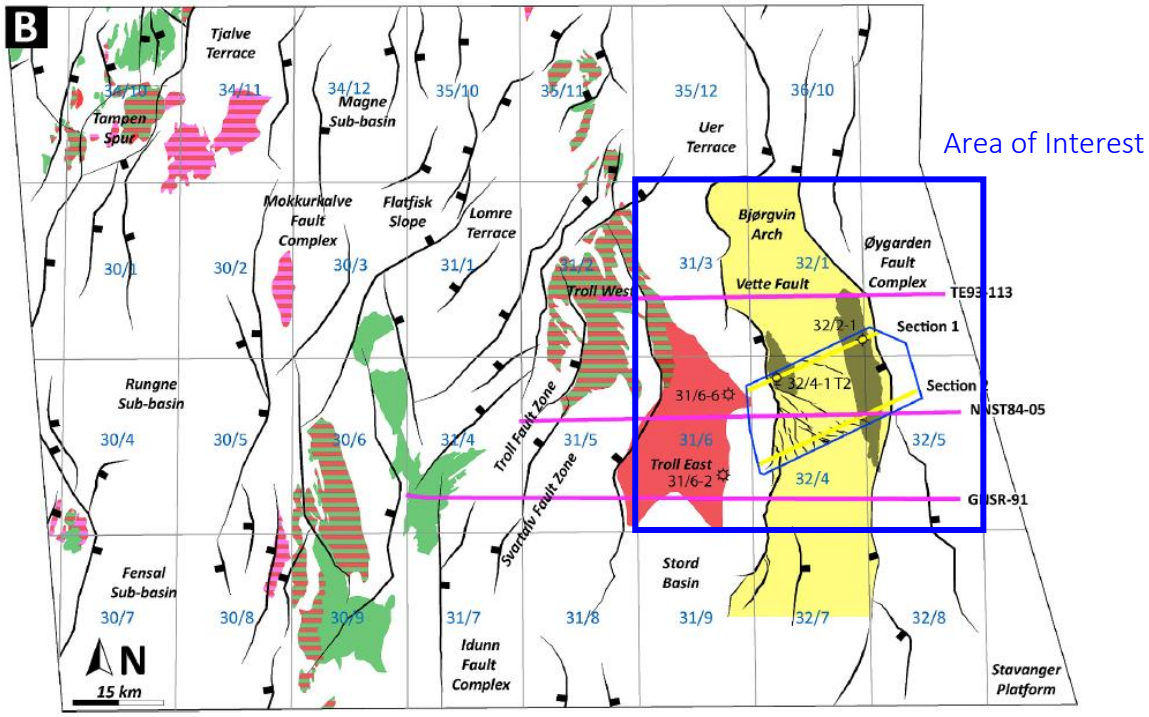

Figure 1-1 Location of investigations within the Northern North Sea, modified after (Mulrooney et al., 2020). *The Primary Area of Interest (AOI) is focused on the Horda Platform and encapsulates the proposed Smeaheia storage site and Troll East field.*

A complete appraisal of the key processes or "drivers" contributing to the stress history can be found in SHARP reports DV1.1a and DV1.1b. Although the region has been subject to major extensional rifting events during the Permo-Triassic and Late Jurassic-Early Cretaceous as

evidenced by the large regional faults (Figure 1-2), the work within this report considers the influence of two of the more recent stress drivers:

- Uplift and erosion – the Horda platform was uplifted during the Neogene by variable amounts. In the East over 1km of sediment was removed and subsequently overlain by Quaternary age deposits.
- Glaciation – expansion of glacial ice into the Norwegian channel has occurred repeatedly over the last ~1Ma, with the last glacial advance between 30 and 10ka bp. Assessment of preconsolidation stresses indicate more significant ice loading in the East (Smeaheia, Troll) relative to the East (Brage, Oseberg).

In subsequent sections the deformation response to these events is simulated. Constraints on loading are based on extensive analysis documented in earlier SHARP reports (DV1.1a, DV1.1b, DV1.2).

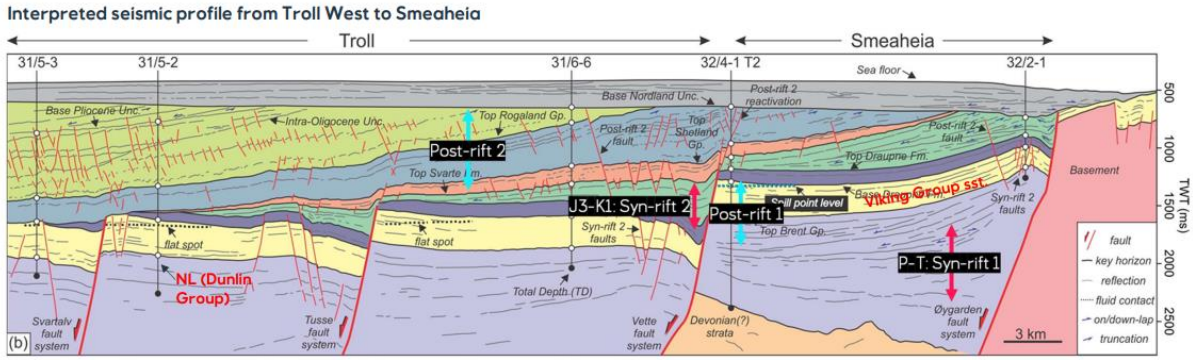

Figure 1-2 Cross section from Troll West to Smeaheia (Wu et al., 2021). *Note the Base Nordland (Quaternary) unconformity highlighting the regional uplift and erosion.*

1.3 Constitutive Modelling Recap – SHARP reports DV1.1b and DV1.2

A focus of this report is understanding *in situ stress* based on knowledge of the *deformation* history. Constitutive models are the link between stress and deformation, and within SHARP DV1.1b a critical-state based constitutive model was introduced for inclusion in predictive modelling workflows. This class of model has been introduced as it provides a unified treatment of volumetric changes with changes in strength (more specifically the preconsolidation strength). The yield surface shape is shown in Figure 1-3(a) and is a function of various constitutive parameters (see DV1.1b), notably but not limited to, the friction parameter β and the pre-consolidation pressure, p'_c. Stress points and associated stress paths are marked with the red dots and arrows respectively. Stress path 1 is within the present yield surface (elastic deformations) and, uniaxial strain boundary conditions, the stress path is only a function of Poisson's ratio, ν. Point 2 is undergoing plastic yielding (normal compaction) and therefore stress path 2 is a function of additional elasto-plastic constitutive parameters e.g. friction parameter, β, which streches the yield surface along the deviatoric stress axis, and the dilation angle, ψ, which controls the relative proportions of plastic shear and volumetric strains (see Crook et al., 2006 for details). Stress path 3 reflects unloading after normal consolidation and as the stress path is elastic it follows the same profile as stress path 1.

Volumetric changes (specific volume) with increasing effective mean stress are shown in Figure 1-3(b). Key parameters in this space are the initial preconsolidation strength, $p'_{c,0}$, the unloading-reloading line gradient, κ, and the gradient of the isotropic normal compression line, λ. Two typical trends are shown; an unaltered specimen (black) showing higher initial porosity, lower initial preconsolidation strength, and more significant volumetric changes under

increasing stress, and a diagenetically altered specimen (blue) showing lower initial porosity, higher initial pre-consolidation strength, and smaller volumetric changes under increasing stress (stiffer deformation response).

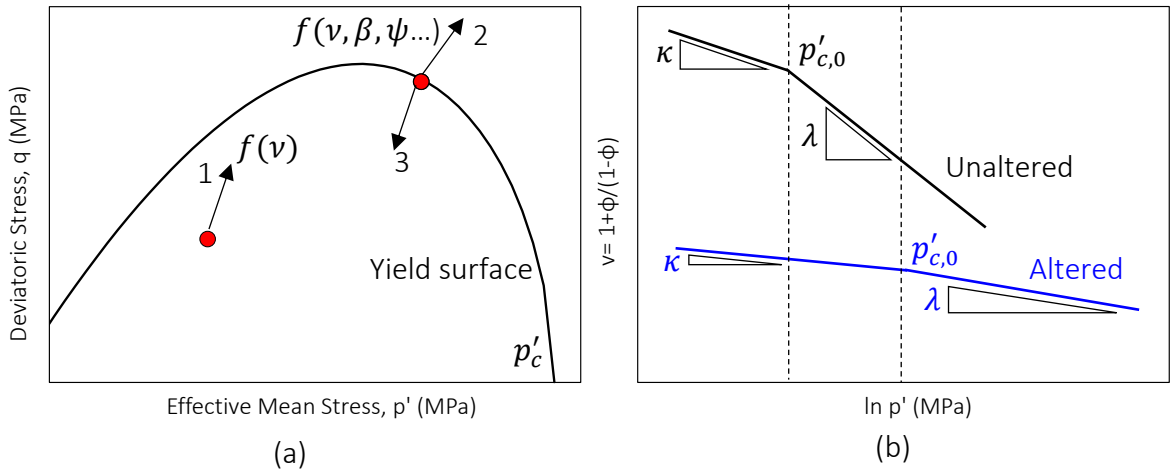

Figure 1-3 Summary of critical-state based SR3 constitutive model (DV1.1b) (a) yield surface shape with potential stress paths (1-3) under uniaxial strain conditions (b) hardening parameters in v-lnp' space – typical responses for both unaltered (mechanical compaction only) and altered (mechanical and chemical compaction) are shown.

Constitutive characterisations for a range of synthetic and natural sediments were developed under DV1.2 based on laboratory data (Grande et al., 2011; Grande & Mondol, 2013). Importantly these explored different clay fractions and clay mineral types (illite, kaolinite, smectite). Constitutive parameters such as those documented above were calibrated such that K_0 and porosity changes during loading and unloading showed satisfactory agreement; Figure 1-4(a,b). The presence of plastic clay minerals such as smectite is known to have significant effect on shear strength, volume changes and K_0. As such further data, such as curves published byWensaas et al., (1998), were used to better understand changes in yield surface profile as a function of smectite content; Figure 1-4(c).

1.4 Structure of Report

The remainder of the report is structured as follows:

- Chapter 2 presents a more generic preliminary investigation that is a continuation of work undertaken in WP1.2 (SHARP WP1.2 Report, 2023) regarding influence of diagenetic processes on *in situ* stress. Extensions to a modelling framework for treating such processes.
- Chapter 3 presents examples of development of stress and pore pressure over geological time at selected locations in the Northern North Sea. The focus area is the Horda Platform area and specifically the Troll East gas field, though the Smeaheia area is also considered due to local variability in the degree of uplift and loading from glaciers.
- Chapter 4 synthesises the model results and considers the significance for risk quantification. Suggestions for integrating the insights into further geomechanical models is provided to assess the degree to which improved stress characterisation effects risk and monitoring requirements.
- Chapter 5 provides conclusions and discussions for areas meriting further investigation.

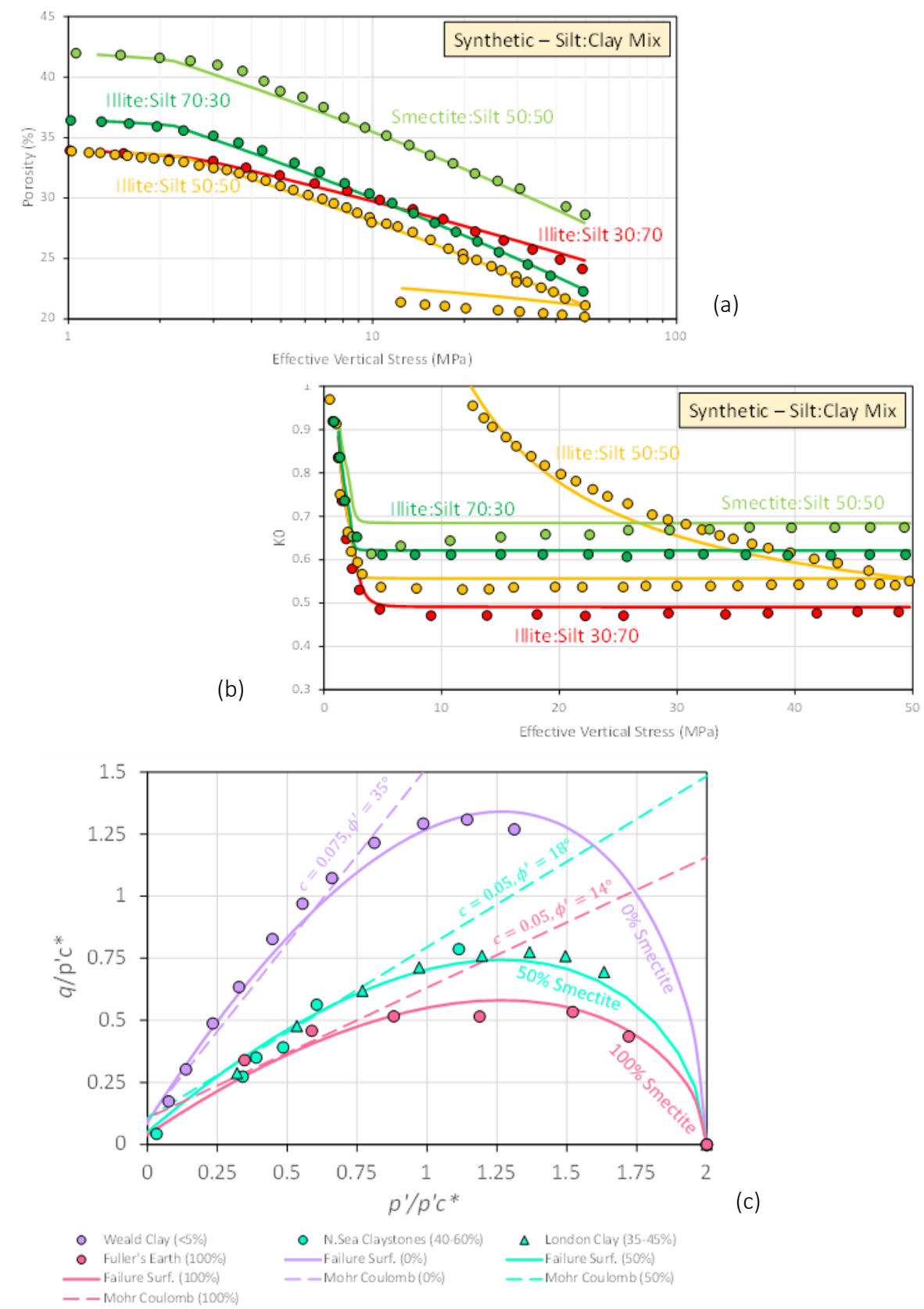

Figure 1-4 Constitutive modelling summary from DV1.2 (a) calibrated hardening for differing compositions and clay fractions (b) calibrated K_0 for differing compositions and clay fractions (c) influence of smectite content on failure surface profile constrained by data in (Wensaas et al., 1998).

2 Assessing the Impact of Burial Diagenesis on Subsurface Stresses

2.1 Overview

A major component of Work Package 1 has been addressing the lithological impact on *in situ* stress as documented in DV1.2. The key aspects of capturing this lithological influence on stress were discussed within DV1.2, and calibrated constitutive models were developed based on mineralogy. This principally focused on mechanical compaction, though an introduction to incorporating diagenesis within the constitutive model was described in earlier reports (DV1.1b). Concisely, this comprised of coupling mechanical porosity changes as determined by the critical-state based constitutive model to chemical porosity changes generated through specific diagenetic laws, which may be basic empirical relationships or published models. These laws aim to capture the *macroscopic* influence of these processes on material state evolution and by extension stress. As part of the previous work in DV1.2 it was noted that several deficiencies in the current implementation could be addressed to meet the objective of better understanding how diagenesis influences *in situ* stress, and these are discussed in the following sections and applied to two relevant caprock shales.

2.2 Conceptual Study of Burial of Draupne and Drake Shales

Following is an investigation of the significance of diagenesis on the primary seals in the Horda Platform area, the Draupne and Drake shales. The description of some relevant extensions to the modelling framework outlined in DV1.1b are discussed at a high level. More detail regarding constitutive properties can be found in SHARP DV3.3.

2.2.1 Extensions to Treatment of Diagenesis

It is widely acknowledged that diagenesis has a significant impact on porosity and sediment fabric (Day-Stirrat et al., 2010) which may in turn effect the evolution of fundamental subsurface properties such as pore pressure (Nordgård Bolås et al., 2004; Schneider et al., 1996). Whilst the influence of diagenesis on sediment stiffness, consolidation characteristics and permeability is documented through laboratory analysis of altered and unaltered rocks e.g. (Nygård et al., 2004), it is generally not trivial to capture the impact of these processes on evolving stress conditions under laboratory conditions. Whilst numerical modelling has the potential to systematically investigate such influence, relatively little attention has been paid to integrating diagenesis into constitutive models to better understand the implications on *in situ* stress. One important recent work in this direction is by Obradors-Prats et al., (2019), in which an extended modified cam clay constitutive model is embellished by linking key constitutive properties to the extent of diagenetic alteration. More specifically the model addresses shortcomings of previous works e.g. Roberts et al., (2014) through:

- Relating parameters such as the gradient of the unloading-reloading line (κ) and isotropic normal consolidation line (λ), which control the bulk material stiffness and hardening characteristics respectively (see Figure 1-3), to the extent of diagenetic alteration. See DV1.1b and DV3.3 for more details regarding these parameters.
- Weighting the amount of strength change due to diagenetic alteration. There is evidence that whilst the preconsolidation pressure in shales may increase through diagenesis it is not as significant as would be predicted from purely mechanical compaction to a comparable porosity (Nygård et al., 2004). Cementation processes in sandstones may result in more significant strength changes however.

The study by Prats and co-workers is particularly useful within the context of the SHARP project as (a) specific attention is given to the Oxfordian age Kimmeridge Clay formation

which is a direct stratigraphic equivalent of the Draupne formation, the primary sealing interval for the Smeaheia area and over much of the Horda Platform, and (b) the computational framework used is similar to the one that will be applied here and was described in DV1.1b (SHARP WP1.1b Report, 2022). The latter means that some of the concepts and approaches can be integrated more or less directly. The computational framework has therefore been modified to include an incremental hardening formulation for the Soft Rock 3 model (Crook, Owen, et al., 2006; Crook, Willson, et al., 2006) with the progressive modification of the material hardening parameters λ and κ during diagenesis following the method of Obradors-Prats et al., (2019). To permit a broader investigation of mineralogical changes this concept is extended to other key constitutive parameters that influence the effective stress ratio K_0 ($=\sigma_h'/\sigma_v'$), notably the parameters β and ψ that control the failure surface shape and dilation characteristics respectively, and Poisson's ratio, ν (Figure 1-3, see also SHARP WP1.2 Report, (2023). The scaling of diagenetic contribution to the pre-consolidation pressure is also handled in the same way as described by Obradors-Prats et al., (2019). The empirical diagenetic model described by Roberts et al., (2014) is retained for simplicity. Application of the model is discussed in the following sections.

2.2.2 Draupne Shale

Here a conceptual study of the evolution of the Draupne formation is undertaken using the extended modelling capability described in the previous section. It is emphasised that the modelling is *demonstrative* with the goal of furthering understanding of how diagenetic processes *may* influence stress conditions. Modelling at the level of a single finite element is appropriate for the applied boundary conditions and is computationally very efficient – the general modelling setup in terms of loading and boundary conditions is shown in Figure 2-1.

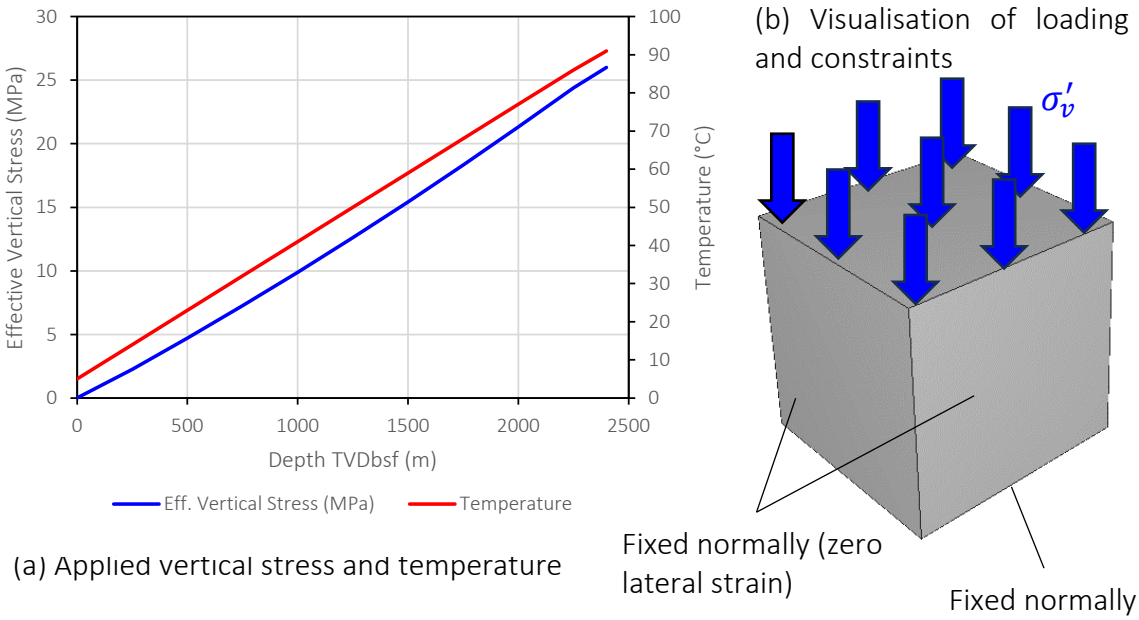

Figure 2-1 Setup of simulation featuring a single 3D hexahedral finite element. Applied stress and temperature conditions are shown together with loading/boundary conditions.

Primary constitutive inputs from the model are derived from the characterisation exercise undertaken as part of DV1.2; a characterisation rich in smectite is adopted (50:50 smectite:silt) to represent the parent material – the friction angle and hardening characteristics are similar to Draupne and unaltered Kimmeridge Clay respectively, even if the smectite content is higher

than typical values for Draupne (10-20% typically).The model aims to target the stress and material state (porosity, mechanical characteristics) reported for Draupne shale from the Ling Depression Soldal et al., (2021)as a detailed description of key mechanical properties is available at this location. The results of the analysis are shown in Figure 2-2. The blue trend shows the replicated porosity evolution with increasing effective vertical stress. Between locations 1 and 2 only mechanical compaction is contributing to porosity reduction. At location 2 the threshold temperature for initiation temperatures is reached (~1.5km) and between here and location 3 chemical compaction dominates porosity reduction. Note that the onset of the diagenetic process is naturally sensitive to the selected initiation temperature of 60°C, which is regarded as a midrange threshold for diagenetic processes in claystones/shales (Bjorlykke & Hoeg, 1997; Day-Stirrat et al., 2010), and the adopted thermal gradient of ~34°C/km (Johnson, 2022). It is worth emphasising that, as evidenced by the extrapolated mechanical compaction trend, porosity reduction to the values indicated for the Draupne Ling Depression sample (15.1%) would require very high effective stresses if considering pure mechanical compaction.

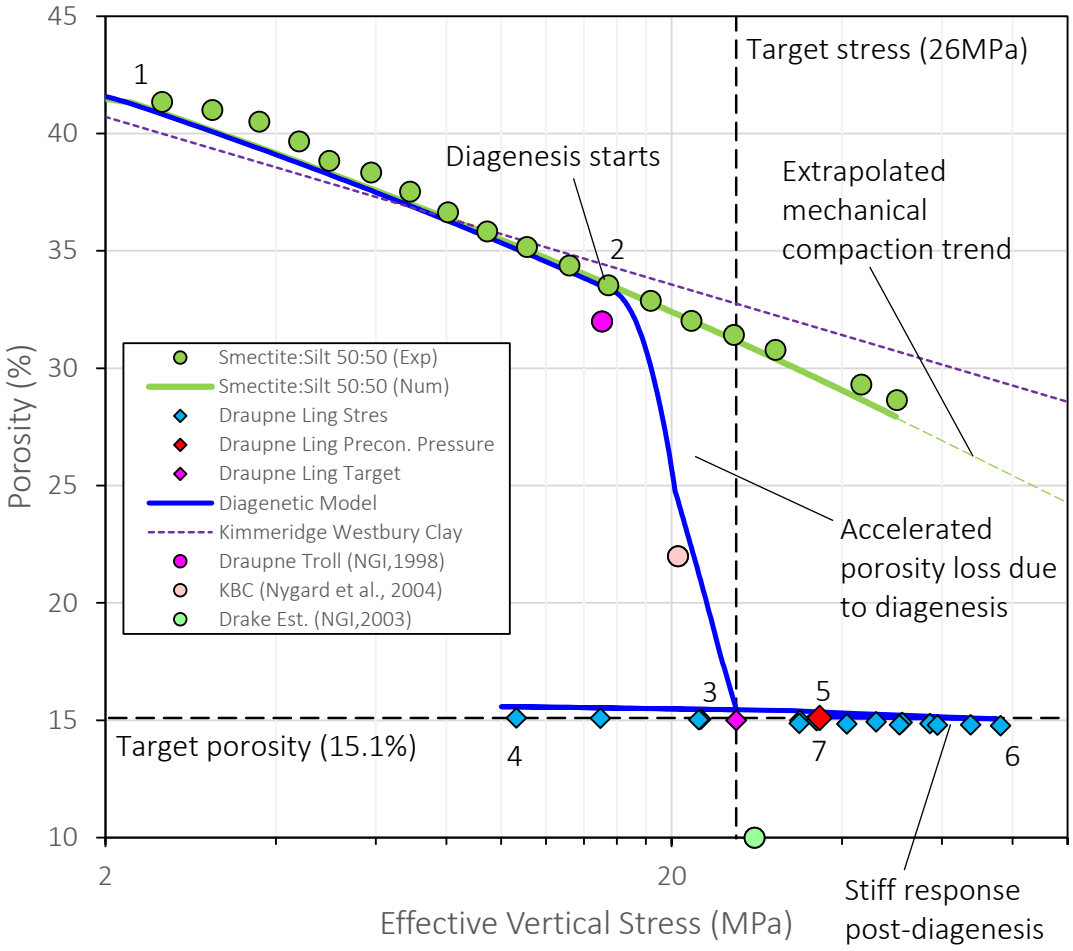

Figure 2-2 Conceptual study showing the simulated evolution of Draupne shale. Upper image shows porosity changes with effective stress with (blue line) and without (green line) diagenesis. The simulation is calibrated to match the porosity and stress conditions at the Ling Depression.

Included on Figure 2-2 are additional reference data points showing the *in situ* porosity and stress conditions for Draupne shale from the Troll field (NGI, 1998) and Kimmeridge Bay Clay (Nygård et al., 2004; Obradors-Prats et al., 2019). These are not used in the calibration *per se* but serve to highlight the accelerated reduction of porosity over a fairly limited range of increasing burial stress once diagenesis starts. Point 3 corresponds to the burial to the *in situ*

effective vertical stress for Draupne shale at the Ling Depression. The simulated porosity at this point is a good match for the experimentally derived porosity value. Similarly to the modelling approach of Obradors-Prats et al., (2019) (refer to their Figure 5) beyond location 3 point we do not permit any further diagenesis and replicate a laboratory testing path performed on the altered material. In this case an oedometric testing stress path reported by Soldal et al., (2021)is simulated. This involved the following loading steps; unloading to σ_v' = 10MPa, reloading to σ_v' = 75MPa, and finally unloading to σ_v' = 35MPa. Note that the deformation response is much stiffer, even after resuming normal consolidation to stresses of 75MPa which is a reflection of the diagenetic modifications to material hardening characteristics. The evolution of K_0 is shown in Figure 2-3(a). Numbering corresponds to the same locations as Figure 2-2. The final K_0 at the end of stress history modelling (location 3) is 0.56. This is somewhat smaller than the reported *in situ* value of 0.66 but is within the range of values observed during experimental consolidation (Zadeh et al., 2017). Unloading from 26MPa to 10MPa between locations 3 and 4 produces a quite significant increase in K_0. The sample is then reloaded to 75MPa between locations 4 and 6, and starts to resume normal consolidation at location 5. The value of effective vertical stress at which normal consolidation resumes is approximately 33 MPa which correlates to an OCR of approximately 1.27. This is close to the reported OCR of 1.38 (Soldal et al., 2021). As the limit of normal consolidation is typically taken to be approximately at OCR of 1.3, a further simulation is undertaken which assumes that diagenetically-induced porosity reduction does not contribute to increased preconsolidation strength increase (i.e. the material is always in a normally consolidated state even when diagenesis is active). The K_0 evolution for this case is shown in Figure 2-3(b). The predicted K_0 is slightly higher at approximately 0.61 which is closer to the reported *in situ* value. The response in unloading results in a slightly higher value. At high stress levels the response is similar to Figure 2-3(a), and the final unloading produces an effectively identical response.

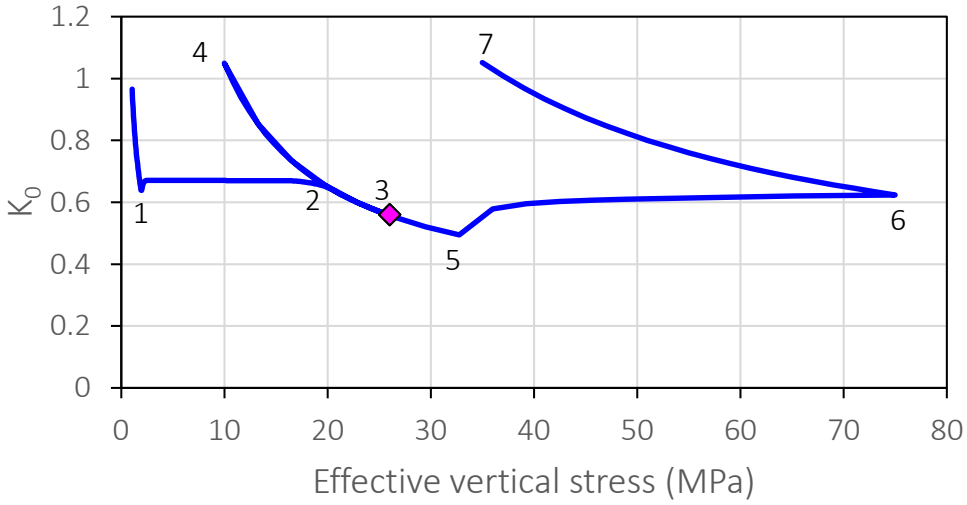

(a) With pseudo-overconsolidation effect from diagenesis

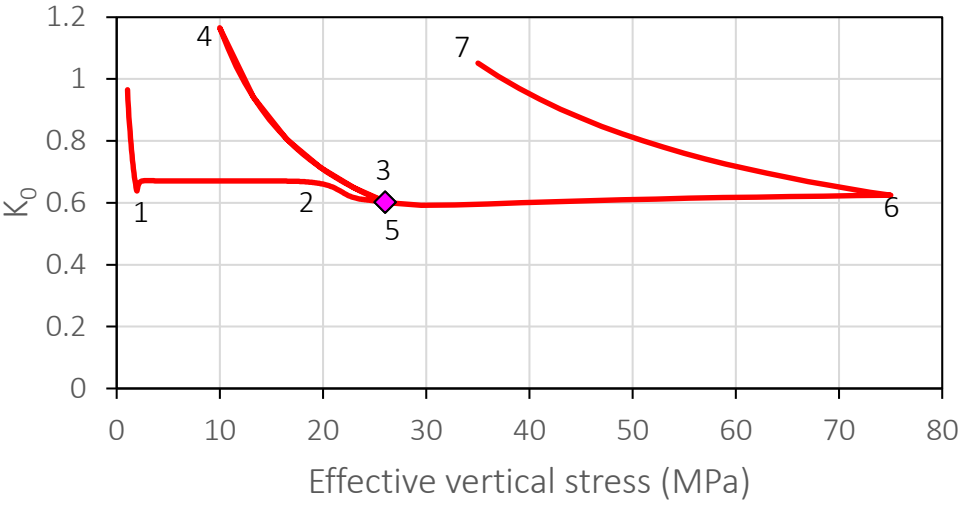

(b) Without pseudo-overconsolidation effect from diagenesis

Figure 2-3 Simulated evolution of K_0 for Draupne shale from the Ling Depression. Two cases are considered – (a) assumes that the light overconsolidation comes from diagenesis and (b) assumes no increase in preconsolidation strength from diagenesis (only normal consolidation). Marker at location 3 indicates that K_0 value at the end of simulating stress history. Between locations 4 and 7 the sample is exposed to laboratory loading conditions reported by (Soldal et al., 2021).

The distinctions between the two representations of the influence of diagenesis during burial are perhaps better illustrated using stress path diagrams in $q - p'$ space (q is the deviatoric stress which reduces to the stress difference $q = \sigma_1' - \sigma_3'$ for triaxial stress states, and p' is the effective mean stress $p' = (\sigma_1' + \sigma_2' + \sigma_3')/3$. Such diagrams are shown in Figure 2-4, and correspond to the same two cases shown in Figure 2-3. In Figure 2-4(a) the pseudo-overconsolidating effect from diagenesis is apparent. Between point 1 and 2 normal consolidation is occurring, the current stress sits on the cap of the yield surface which is expanding as porosity is reduced. Beyond point 2 diagenesis is active and at maximum burial depth (point 3) the stress path is *not on the yield surface*. The term 'pseudo-overconsolidating' is well illustrated here as it could be assumed, for instance, that the material was in fact normally consolidated to point 5 and then overconsolidated to point 3, whereas in fact point 3

represents the maximum burial depth and the increase in pre-consolidation strength is a result of chemical processes. The stress path is steep between points 2-3 (and also during subsequent unloading from 3 to 4 and re-loading 4 to 5) because the strengthening results in an elastic response. Note that the behaviour in Figure 2-3Figure 2-4(b) is quite different and because the strengthening effect of diagenesis is not modelled the stress point at maximum burial is on the yield surface.

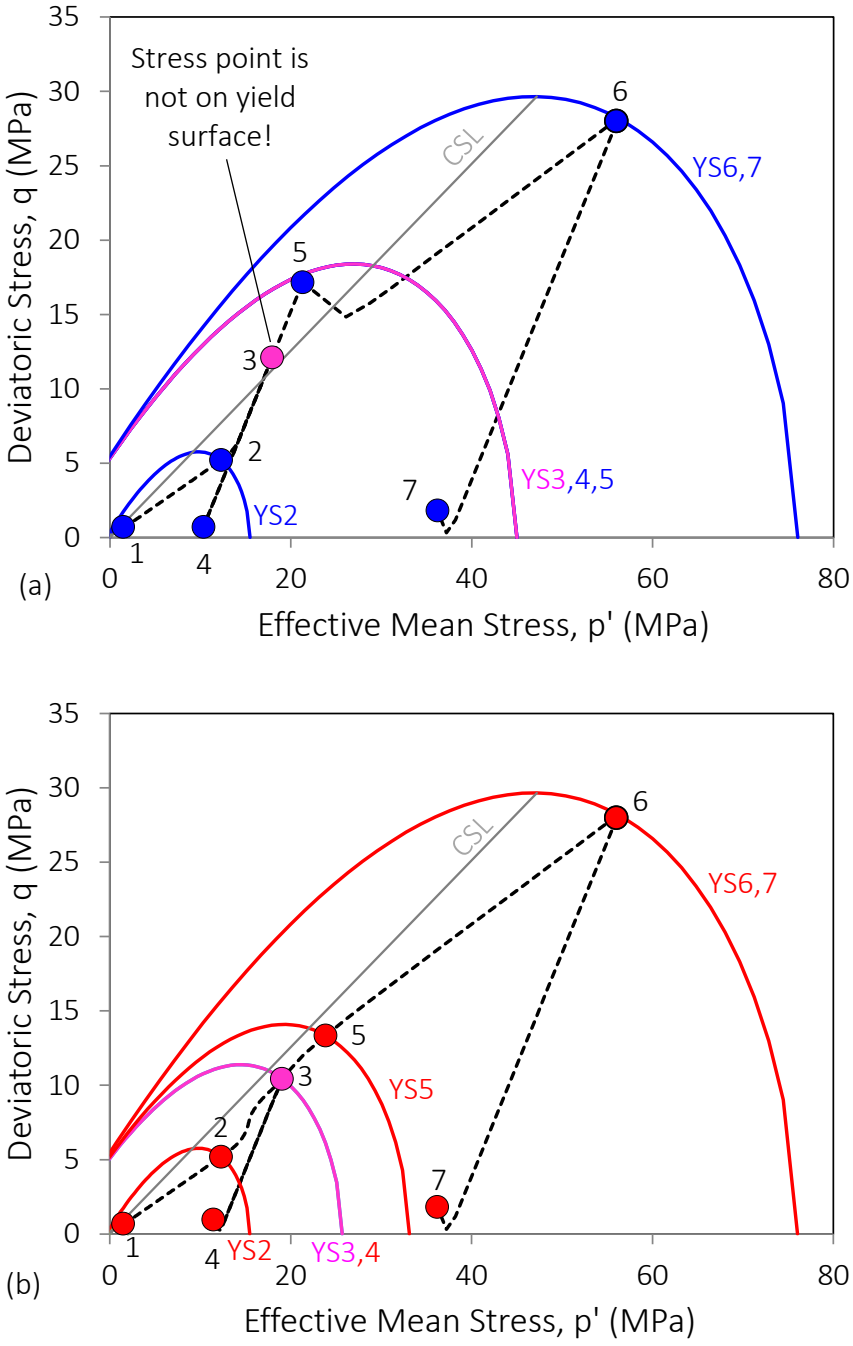

Figure 2-4 Stress paths in q-p' space (a) with pseudo-overconsolidation from diagenesis (b) without pseudo-overconsolidation from diagenesis. Stress path is shown with black dotted line, and filled circles represent stress state at points corresponding to those shown in Figure 2-2 and Figure 2-3. YS represents the yield surface for the specific stress state(s).

Turning attention to the Area of Interest (AOI) in the Northern North Sea, we assume that the same generic characterisation of the diagenetic process developed for the Draupne formation at the Ling Depression is representative here. As diagenesis can be very site specific owing to variations in composition, pore fluid chemistry and burial/temperature conditions the validity of this assumption may be questionable, and this is discussed at a later stage. Experimental data for Draupne shale at the Troll field (NGI, 1998) at least indicates that the change in K_0 during elastic consolidation is satisfied by a Poisson's ratio of 0.2, which is the same as reported for the Draupne shale at the Ling Depression. We also assume similar the same basic effective vertical stress input (Figure 2-1) to derive loading histories for two wells from the Horda Platform; 31/6-1, 32/2-1, and 31/5-7 from the Troll East, Smeaheia Beta and Aurora areas respectively. The effective vertical stress change correlates well with estimates developed earlier in the SHARP project (SHARP WP1.2 Report (2023, Figure 2-11). For temperature we increase the thermal gradient to 40°C/km at Smeaheia Beta following Rahman et al., (2022). The Draupne formation at the Troll well has been subject to a relatively shallow burial with an estimated maximum burial depth of ~1400m followed by uplift of 400m, whilst at Smeaheia Beta the burial depth is greater (~1800m) and the uplift is much larger at approximately 1300m (DV1.1b, DV1.2).

The simulated stress histories are shown in Figure 2-5. For the Troll well, which has not been deeply buried, the final reported K_0 value is predicted to be 0.855 which agrees quite well with the value of 0.87 determined from Leak-Off Pressures (LOP) from Grande et al., (2022). The final porosity for this well is very slightly overpredicted (34% predicted versus 32% observed). For the more deeply buried and uplifted Smeaheia Beta well the final K_0 is overpredicted, with a simulated value of 1.45 being somewhat larger than the value of 1.25 indicated by LOP (Grande et al., (2022) . It is perhaps significant that this sample has been more buried relative to Troll, and has potentially been more affected by diagenesis. It was noted in DV1.2 that altered samples appear to be less affected by uplift. This is also reinforced by the values reported from Smeaheia Gamma well, which is the most deeply buried at around 1900m but has also been uplifted by approximately 1000m. The value of K_0 at the Smeaheia Gamma well is between 0.54 and 0.6, as determined from XLOT and LOP respectively. Note that there is higher confidence in the K_0 derived from XLOT compared to LOP, and there is some uncertainty in the interpretation of the high LOP of 1.25 at Smeaheia Beta as raw data cannot be assessed. This is hard to reconcile with the simulation of the Beta well which shows significant increase in K_0 but broadly similar maximum burial depths and uplift. One explanation could be that material properties exhibit some significant variability both horizontally and laterally, leading to differing responses under both loading and unloading. This seems quite probable. For instance, variability in Poisson's ratio was shown to be significant in predicting unloading responses (SHARP WP1.2 Report (2023), Chapter 4). Furthermore, the Draupne shale is known to be quite complex due to the high organic content and this is discussed later within this chapter.

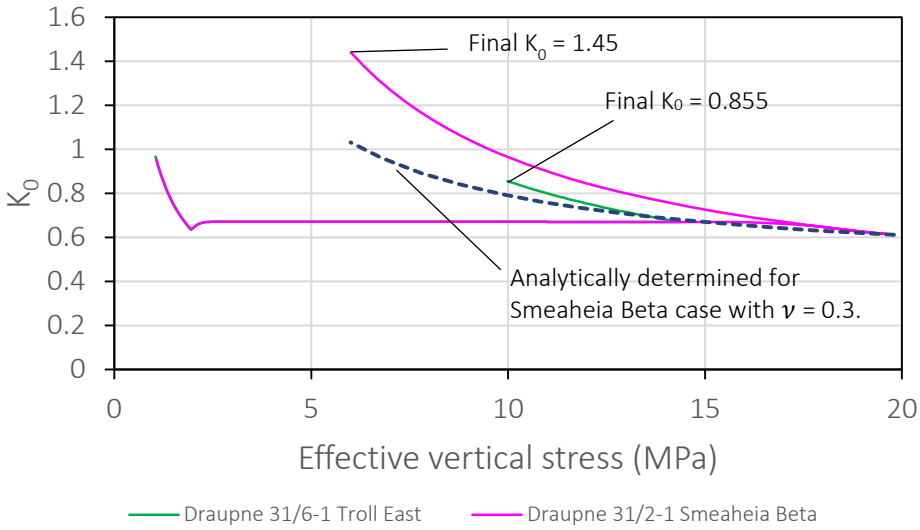

Figure 2-5 Predicted stress histories for Draupne formation in the Horda Platform area accounting for mechanical and chemical compaction and subsequent uplift. The final reported K_0 values for the Draupne shale are 0.855 and 1.45 for Troll and Smeaheia Beta respectively.

2.2.3 Drake Shale

A similar modelling process can be followed to investigate the evolution of the Drake shale. Conditions at the Aurora well are simulated, where the overburden loading profile from Figure 2-1(a) is retained but the thermal gradient is modified to 34°C/km (Rahman et al., 2022). The maximum burial depth is of the order 2500m and uplift is estimated to be approximately 300m (DV1.2). Mineralogically, the Drake formation has a high quantity of illite (Thompson, Andrews, Wu, et al., 2022) and it is assumed here that initially the sediment contained a higher quantity of smectite. The same generic diagenetic model used for Draupne shale is applied and the more significant burial depth results in increased porosity reduction. This also agrees quite well with the recorded porosity of around 10% for Drake Shale (Griffiths et al., 2023) as shown in Figure 2-6(a). The evolution of K_0 for scenarios with and without diagenetic strength increases (pseudo-overconsolidating effect) is shown in Figure 2-6(b) Figure 2-6(c) respectively. In each case multiple values of Poisson's ratio are simulated which bound the range of values observed and reported for the Drake formation (SHARP WP1.2 Report, 2023; Thompson, Andrews, Wu, et al., 2022). In both (b) and (c) it can be noted that modifying Poisson's ratio does have some influence on the K_0 value under normal consideration. Changes in K_0 once temperatures sufficient to initiate diagenesis are reached are shown in (b) to be more pronounced, particularly when Poisson's ratio is lower. This occurs because the strength increase arising from diagenesis is sufficient to increase the size of the yield surface more quickly than changes in stress through burial (see equivalent behaviour for Draupne formation in Figure 2-4(a)). The response is therefore elastic and under assumptions of material isotropy changes in K_0 during unloading (ΔK_o^{iso}) are determined by Eq.1
:

$$\Delta K_o^{iso} = \frac{\nu}{1-\nu} \qquad \textit{Eq. 1}$$

Therefore, the K0 tends to lower values for lower Poisson's ratio. As the stress path from onset of diagenesis results in an elastic response, the stress path during uplift from maximum depth to present depth (marked with triangular symbols) follows the same path. For low Poisson's

ratio values the final K_0 is within the upper range of values indicated from XLOT and LOP (marked with yellow square symbols).

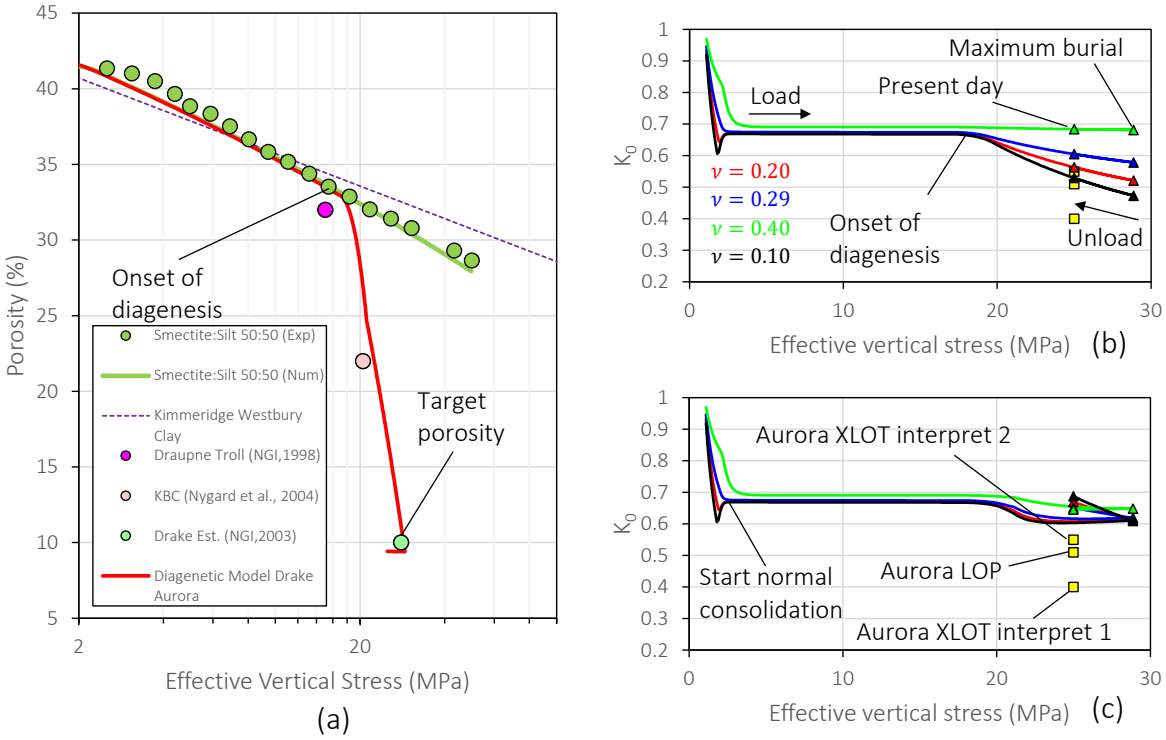

Figure 2-6 Simulating burial and minor uplift of Drake Shale representative of the Aurora well (a) Porosity changes with burial and uplift (b) Evolution of K_0 with pseudo-overconsolidation effect from diagenesis (c) Evolution of K_0 without pseudo-overconsolidation effect from diagenesis. In both (b) and (c) different values of Poisson's ratio are explored in the range [0.1, 0.4]

Equivalent simulations assuming that diagenesis does not significantly alter strength i.e. sediments are always normally consolidated is shown in Figure 2-6(c). After onset of diagenesis the reduction in K_0 is a result of the modification of hardening and stiffness variables as these are retained from the Draupne characterisation. Unloading responses in this scenario result generally in increase of K_0 which becomes less significant for higher Poisson's ratios. The predicted values after uplift are higher than indicated by the *in situ* stress measurements. However, some key constitutive properties still reflect a sample that has a high smectite content and without considering the gradual transformation of smectite to illite during diagenesis. This is addressed in Figure 2-7(a) where processes such as the smectite-to-illite transformation are modelled so that during diagenesis the progressive transition of friction and dilation angles from smectite-rich properties i.e. characterisation 50:50 smectite:silt (SHARP WP1.2 Report, 2023) to higher proportions of illite is treated. Specifically, the 50:50 illite:silt characterisation is used to define target properties after completion of the diagenetic process with additional constraint on the friction angle for reconstituted Drake material equal to 26.8° (SHARP WP1.2 Report, 2023; SHARP WP3.2 Report, 2023). The base case (red curve) predicts K_0 at maximum and present depths of 0.61 and 0.65 respectively, giving ΔK_o = 0.033 during unloading. Accounting for the friction and dilation changes during diagenesis (Variation 1, black curve) results in K_0 values at maximum and present depth of 0.525 and 0.542, giving ΔK_o = 0.017 during unloading. The final K_0 in this case agrees quite well with the LOP and one XLOT interpretation (0.51 and 0.55 respectively). Importantly, this shows that under the

stated assumptions (a) the K_0 during normal consolidation may be lower due to diagenetic processes and (b) the change in K_0 during unloading will be smaller as a result of the reduced K_0 at maximum burial (SHARP WP1.2 Report, 2023). To this point all modelling has been performed under the assumption of material isotropy. However, the Drake formation is known to be highly anisotropic based on experimental testing (Griffiths et al., 2023). The stiffness in the direction parallel to bedding is over 5 times higher than normal to bedding (Table 2-1).

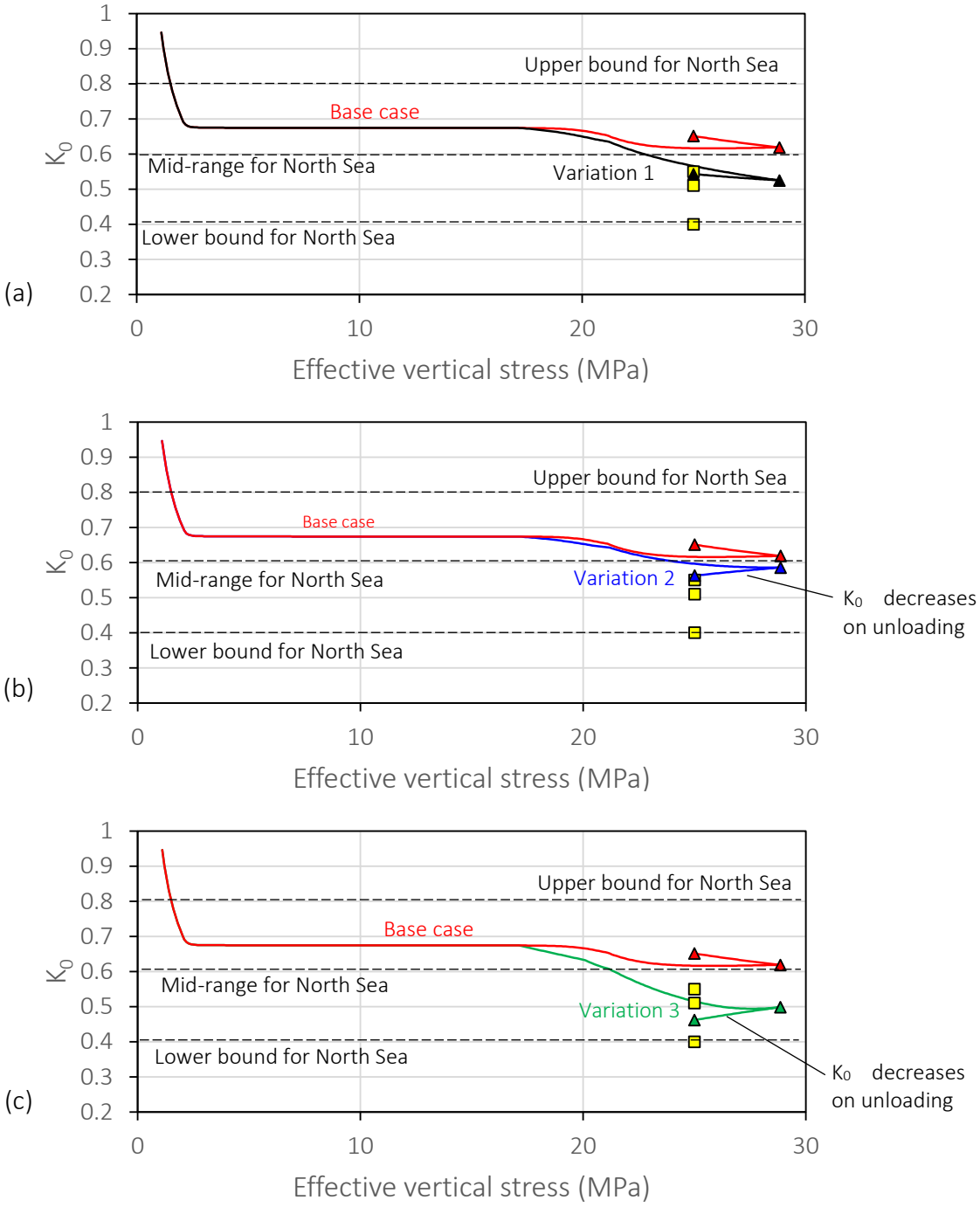

Figure 2-7 Further simulations of burial and minor uplift of Drake Shale representative of the Aurora well under normally consolidated conditions (a) Consideration of simulating transformation of fundamental properties such as friction and dilation angle as a function of diagenetic alteration (b) Simulating increase in Poisson's ratio from 0.29 to 0.42 during

diagenesis to reflect progressive anisotropy development (c) Variation of (b) where change in friction/dilation is more rapid and Poisson's ratio changes through anisotropy develop later. Upper and lower bound K_0 values for North Sea are shown for reference (based on observed variation range of XLOT tests, see Andrews & de Lesquen, 2016 and also SHARP reports DV1.2 and DV3.2).

E_v (GPa)	E_h (GPa)	E_h: E_v*	ν_v (-)	ν_h (-)	ΔK_o^{vti} (-)	ν_{iso} (-)
3.85	22.47	5.83	0.09	0.29	0.738	0.424

*Table 2-1 Properties for Drake Shale established through drained triaxial testing (Griffiths et al., 2023). Note the significant differences in reported values depending on the sample orientation. * Reported anisotropy ratio based on values reported during unloading. For values taken during loading the implied anisotropy is greater than 7.*

For a vertically transversely isotropic (VTI) medium the change in K_0 during unloading is given by (Andrews & de Lesquen, 2019):

$$\Delta K_o^{vti} = \frac{E_h}{E_v}\left(\frac{\nu_v}{1-\nu_h}\right) \qquad \text{Eq. 2}$$

So, in this case there is a consideration of Poisson's ratio measured normal and parallel to bedding (ν_v and ν_h respectively) and Young's modulus for the equivalent orientations (E_v and E_h). Table 2-1 shows that the value of ΔK_o^{vti} from Eq.2 is 0.738. Also shown is the value of ν_{iso}, which represents the value of Poisson's ratio necessary to obtain the same ΔK_o under the assumption of material isotropy, which is equal to 0.424. This is explored in Figure 2-7(b), again under assumptions of material isotropy, where in addition to the changes to friction and dilation angles, Poisson's ratio (ν) is modified from the initial value of 0.29 to the value of 0.424 (Variation 2, blue curve). By comparing this to the results for Variation 1 it is clear that increasing the value of Poisson's ratio (ν) has the effect of increasing K_0 during normal consolidation. However, importantly the elevated Poisson's ratio results in a decrease in K_0 during unloading, resulting in a final K_0 of 0.563. As this indicates that the changes in properties can appear to cancel each other out, the requirement for the processes to occur synchronously as a function of the degree of diagenesis is relaxed in Variation 3 – green curve, Figure 2-7(c). This simulation permits a more rapid modification of friction and dilation characteristics, but Poisson's ratio changes due to anisotropy occur at a later stage. The assumption of relatively late anisotropy development could be justifiable e.g. Worden et al., (2005), their Figure 9b which shows modest fabric anisotropy until the relative proportion of illite is quite high. Under these assumptions the lowest K_0 values which are 0.498 and 0.462 at maximum burial and present conditions respectively, giving ΔK_o = -0.036 during unloading. This scenario approaches the low XLOT interpretation.

2.3 Summary

The modelling within this chapter has leveraged the mineralogy specific constitutive characterisations developed as part of Task 1.2 to explore the possible influence of burial diagenesis on stress development during both burial and exhumation. The main outcomes and findings of the chapter may be summarised as follows:

- Additional functionality has been incorporated into the existing diagenetic constitutive models to permit changes to hardening characteristics following published

methodologies. These concepts have been further extended to permit changes to other variables that influence K_0 such as friction/dilation parameters and Poisson's ratio. It must be emphasised that diagenetic model is, by design, very simple but the processes it seeks to represent are invariably complex.

- The extended functionality has been used to study potential stress evolution of Draupne shale through the application of a simple empirical diagenetic model, calibrated using experimental data from the Draupne shale sampled from the Ling Depression. The implications of diagenetically-sourced pseudo-overconsolidation on the stress path were demonstrated. Application of this characterisation to Troll data showed good correlation to in situ K_0, whilst application at Smeaheia Beta exhibited an overestimation of K_0 on unloading.
- Application of the same basic empirical diagenetic model to the Drake shale showed reasonable correlation to *in situ* porosity given the simplified representation of the burial and thermal history. This was used to explore the significance of various constitutive parameters under assumptions of normal consolidation and pseudo-overconsolidation from diagenesis, providing a range of possible responses.

The analyses undertaken provide the following key insights in terms of in situ stress determination for deeply buried and diagenetically altered sediments:

- The results suggest that diagenesis induces changes to sediment properties that reduce K_0 during normal consolidation. This statement holds irrespective of whether the overconsolidating effect (strength increase) from diagenesis is considered or not. This is compatible with experimental observations (Nygard et al., 2004).
- As shown and discussed in DV1.2 a reduced K_0 at the end of burial will result in less-sensitivity to K_0 changes during unloading, and this appears compatible with *in situ* observation and experimental observations (DV1.2, DV3.2).
- The contribution of diagenesis to preconsolidation strength is an important aspect as this was shown to provide quite distinct behaviours cf. Figure 2-6(b) and Figure 2-6(c). However, due to the large disparity between experimental loading rates and *in situ* loading rates it can be difficult to determine whether the reported yield stresses in experiments reflect the *true* yield stress. As discussed by Ewy et al., (2020) it is possible that yielding of shales may be observed at lower stresses if experiments are performed at significantly reduced rates. Potentially for some sediments/reactions the overconsolidating effect is less pronounced and the current stress state always lies on the yield surface during burial. This is further complicated by the subtleties of different processes and contribution of cementation.
- The influence of anisotropy has been examined in a very simplified way. However, this was shown to potentially have a profound impact on unloading behaviour. More deeply buried shales which may have undergone transformation of smectite to illite, such as Drake, could feature very strong anisotropy. There is experimental evidence to support this strong anisotropy in the Drake formation (Table 2-1). For VTI materials this was shown to influence the change in K_0, and through simulation resulted in a strong decrease in K_0 on unloading. Whilst fabric development and anisotropy may develop during mechanical compaction of shales, it may become more pronounced as a result of deeper chemical processes e.g. illitisation (Charpentier et al., 2003; Worden et al., 2005).

3 Significance of Stress History on *In Situ* Stress and Pore Pressure – Assessment at the Troll Area, Horda Platform using Forward Geomechanical Modelling

3.1 Introduction

This section addresses the importance of stress history in terms of developing predictions of present *in situ* stresses. Investigations within the DV1.2 report indicated some areas of uncertainty that merited further exploration through geomechanical modelling. Specifically, shallow Leak-Off Pressures (LOP) in the Tertiary units at Troll indicated higher than anticipated horizontal stresses. The source of this is uncertain and could result from:

(a) Some residual overpressure that provides an elevated Shmin and implies a high K_0 value if hydrostatic pressures were assumed, or

(b) The presence of plastic clays which have high K_0 values under normally consolidated conditions (Grande et al., 2022).

The work documented within this section aims to address these questions through geomechanical forward modelling. Via this approach the important elements of the stress history can be represented explicitly and the implications of these processes for present stress and pressure conditions can be systematically investigated. The Troll East 31/6-1 is relevant to CO_2 storage in the region and has been selected as:

- It is in close proximity to regional storage targets (Aurora, Smeaheia).
- It is a data-rich location. The shallow 200m has been subject to detailed shallow-geotechnical investigations previously (Lunne et al., 2006) and within SHARP (Jalali, 2022; Kopperud & Myhrvold, 2023; SHARP WP3.2 Report, 2023). Stresses have been assessed at more significant depths within the project also (Grande et al., 2022; SHARP WP1.2 Report, 2023).

3.2 Modelling Methodology

The computational modelling framework has been described previously (SHARP WP1.1b Report, 2022)and relevant publications (Peric & Crook, 2004; Thornton & Crook, 2014) and so only key details are outlined here. The models employ a coupled finite element modelling framework that incorporates adaptive remeshing algorithms, which are essential for this application to treat topology changes arising from deposition and/or uplift. Constitutive models applied are based on characterisation efforts documented in (SHARP WP1.2 Report, 2023) for the Soft Rock 3 (SR3) material model (Crook, Willson, et al., 2006) – see also summary in Figure 1-4.

3.3 Troll East Well 31/6-1

3.3.1 General Model Setup

The forward geomechanical model begins with a nominal base layer representing the base of the Tertiary section. Stress and pore pressure conditions are initialised within the layer compatible with the normally consolidated K_0 value and assumed hydrostatic pore pressure. Boundary conditions are imposed such that the model base is fixed in the vertical direction and the lateral boundaries are fixed in the horizontal direction. The lateral boundary conditions are important and reflect conditions of *zero lateral strain*. These conditions are considered to be representative of passively subsiding sedimentary basins and are compatible with assumptions

that underpin log-based stress characterisation workflows developed earlier in the SHARP project (Grande et al., 2022; SHARP WP1.2 Report, 2023). Sedimentation and erosion algorithms are used to define the addition and removal of sediments and automatically establish the required load cases.

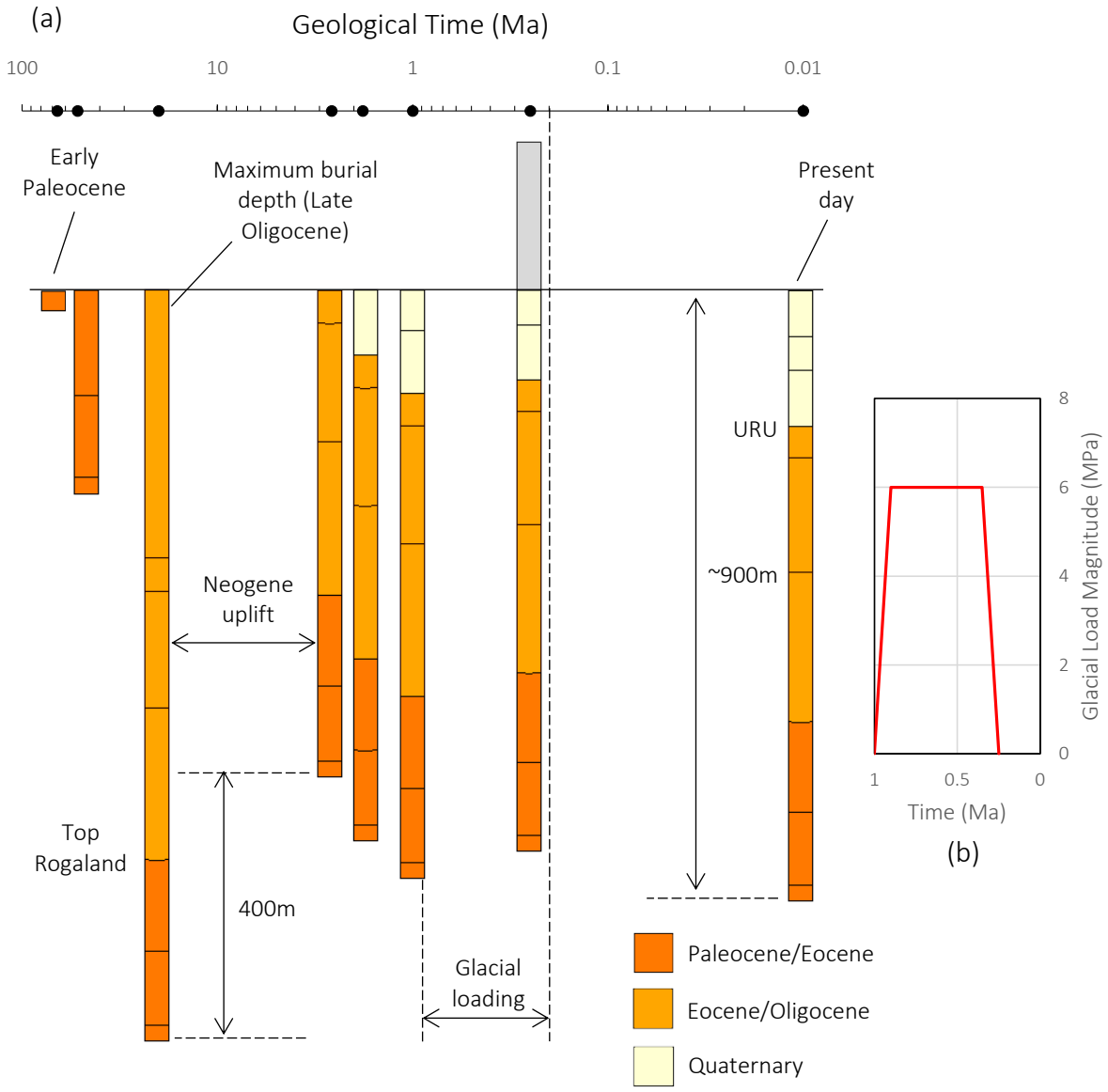

Figure 3-1 Setup of 1D forward geomechanical model assessing conditions in Tertiary and quaternary age sediments at the location of the well Troll 31/6-1 (a) simulated loading history (b) simplified ice loading curve during quaternary. Note a logarithmic scale is used as many geological events simulated occur within the last 3Ma.

Ice loading is represented via application of a face load equal to the weight of the ice which, whilst uncertain, is suggested to be approximately 6.0MPa based on understanding derived in Task 1.2 (SHARP WP1.2 Report, 2023, Figure 2-11). The appropriate application of the loading is uncertain – in reality there will have been periodic advance and retreat of glaciers. Loading is simplified here and is ramped to maximum value over 0.1Ma to simulate glacial advance, held for 0.65Ma and then reduced over 0.1Ma to represent the glacial retreat which completes by 25ka bp.

3.3.2 Modelling of Secondary Sealing Units (Tertiary)

Calibration data is derived from well reports (npd.no) and published data (Grande et al., 2022). It is necessary to homogenise/upscale as it is impractical to incorporate the significant vertical heterogeneity that is evident in the log data. As such, two simplified versions of the K_0 trends determined by Grande et al., (2022) based on clay fraction are shown in Figure 3-3(a). These reflect the calculated K_0 both with and without stress history correction. The uncorrected curve is used as a basis for material property assignment.

The setup for the base case (Simulation A) is as follows:

- The *illite:silt 50:50* characterisation is used as a foundation as the unloading behaviour for this sample was well constrained – matched with Poisson's ratio of 0.29 (SHARP WP1.2 Report, 2023), and it represents a typical clay fraction. Due to the fact that the laboratory testing was undertaken on samples already consolidated to 2MPa the characterisations are assigned a higher depositional porosity, with pre-consolidation strength adjusted automatically.
- For the lower portion of the Tertiary sedimentary package (>750m) the friction parameter is adjusted to account for the observed clay fraction of ~60%; Figure 3-2.
- A similar procedure is adopted for the upper portion of the Tertiary which has a representative clay fraction of around ~47%; Figure 3-2.
- Just below the unconformity a small sand sequence (~50m thick) is indicated in the logs and this is represented in the model using the *QA sand* characterisation (SHARP WP1.2 Report, 2023).
- The material hardening characteristics, with the exception of the sand interval below URU, are the same for all materials. The hardening trend from the *smectite:illite 50:50* characterisation is found to be a good general fit to the logged bulk density profile. Establishing representative hardening is important as volumetric strain development during compaction is used to update sediment porosity and by extension any porosity dependent parameters like bulk density. Hence the recovered stress profile is closely linked to the compaction behaviour.
- The quaternary sediments are not the focus of this investigation but are represented similarly. For units I/II, III and IV the value of Poisson's ratio is increased to 0.33, which represents the average value reported for quaternary sediments (see (Jalali (2022), Table 9-2) – the documented values appear to have been derived based on *in situ* K_0 (via rearranging Eq.1), and so further constraint based on experimental testing would be useful in future. The value of 0.33 broadly correlates with the range inferred from K_0 testing on shallow mudstones (<1km burial) documented in WP1.2 (SHARP WP1.2 Report, 2023, Figure 3-24).

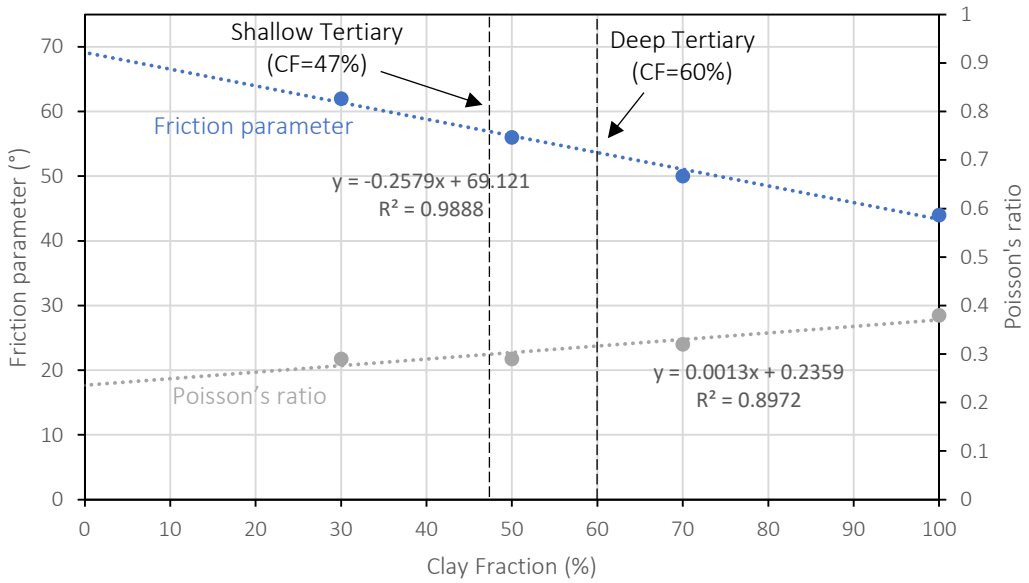

Figure 3-2 Synthesis of relationships between key constitutive parameters and clay fraction following characterisation efforts in SHARP Task 1.2. Caution: friction parameter is not the same as friction angle as it is defined in a specific stress space (q-p'). See DV1.1b report for definition.

The results of the model are interrogated through depth and the simulated K_0 for the Simulation A is shown in Figure 3-3. Encouragingly the predicted K_0 shown in (a) is generally a good match for the log-based trend. This provides some confidence in wider application of the developed characterisations for simulating stress history influence on shallow sediments in the northern North Sea in particular. It is emphasised that in the Tertiary the model has *not* been specifically calibrated beyond ensuring the vertical total stress is comparable to observations (through selection of hardening) and by making minor corrections to the base characterisation depending on known clay fractions. The appropriate hardening inputs are confirmed by the comparison in (b), where despite there being some variability in the log data the general trend of sediment bulk density with depth is captured well in the model. Whilst additional work could focus on more detailed representation of stratigraphy and more precisely capturing the variation in material properties such as density it is not likely to add significant value to the modelling exercises at this stage.

The significance of capturing the stress history component is shown in Figure 3-4 which shows the changes in (a) effective vertical stress and (b) K_0 ratio at various times through the simulation. Note that model indicates the distribution of K_0 over geological time is variable. For instance, larger values predicted when the sediment becomes overconsolidated following the Neogene uplift, but magnitudes then drop due to resumed normal consolidation from emplacement of quaternary sediments and ice loading, before increasing again as the glacier retreats. This behaviour would likely vary across the Horda Platform owing to different relative amounts of uplift and ice loading (SHARP WP1.2 Report, 2023, Figure 2-11). At Smeaheia it is likely that the more significant uplift could have been extensive enough for consolidation not to have resumed i.e. following uplift any additional loading was expressed elastically. Future investigations aiming at assessing more wells could be undertaken relatively easily. At locations such as Troll West and Oseberg uplift is more modest and ice loading would have probably resulted in resumed normal compaction, as observed at Troll East.

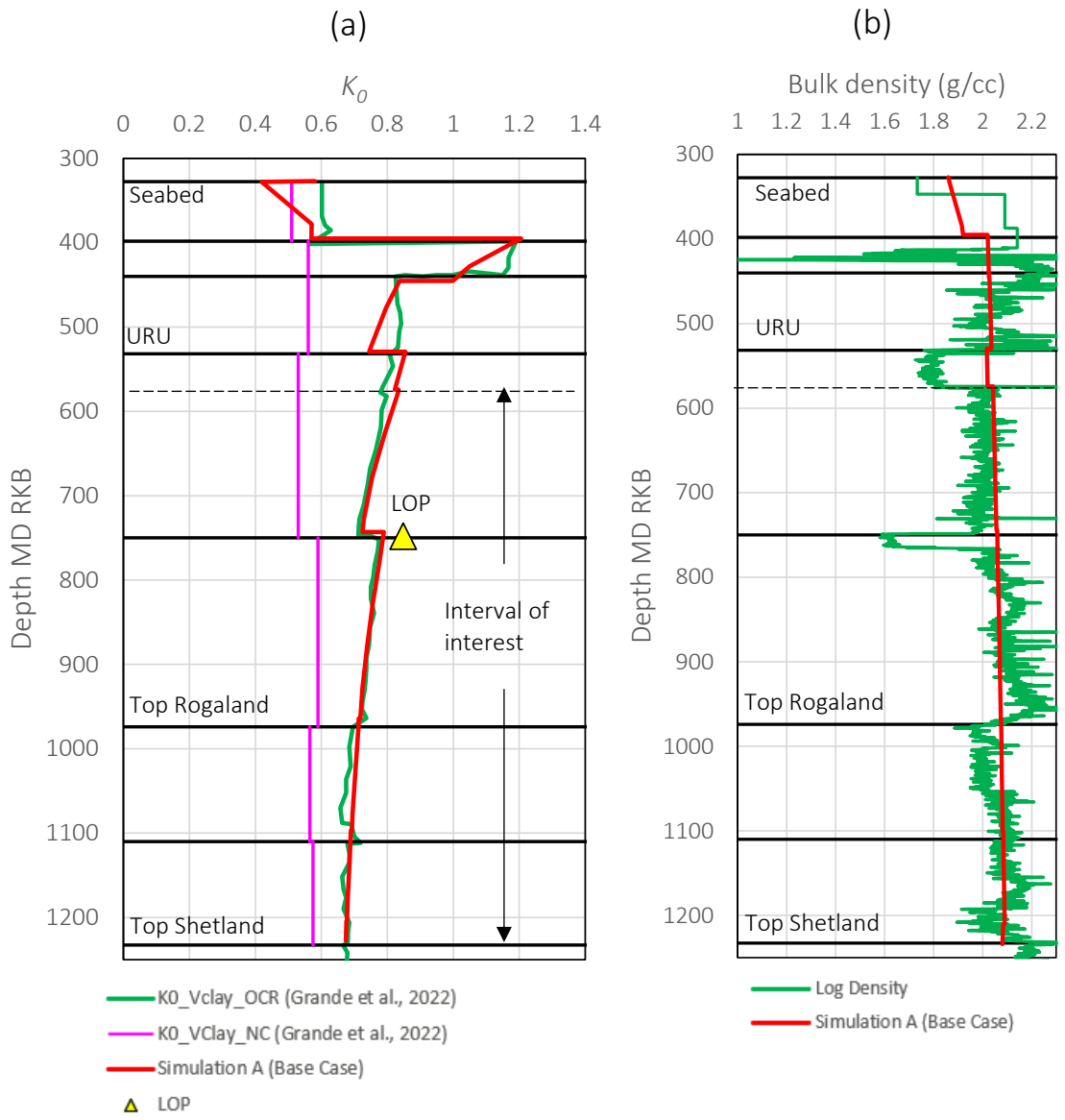

Figure 3-3 Comparison of simulated output and log-based trends for Troll East well 31/6-1 under base case conditions. (a) K_0 variations with depth (b) density variations with depth. Note log based K_0 trends are simplified versions of the published data.

3.3.1 Exploring Uncertainties in the Secondary Seals

As noted in the previous sections there exists some uncertainty with respect to precise sediment composition and drainage characteristics in the Tertiary age sediments, and how these aspects might contribute to the relatively high LOP measurement. Firstly, the presence of smectitic and plastic claystones in the lower Tertiary is explored – hereafter referred to as Simulation B. This comprises of making additional adjustments to the sediments in this region to account for the different mineralogy. Based on the constitutive modelling study of smectitic claystones (SHARP WP1.2 Report, 2023, section 4.2.3) an estimation of the required changes can be made – for Poisson's ratio and friction parameter the relationship is summarised in Figure 3-5. Combining this information with suggested smectite fraction for Hordaland Group at nearby Troll West (25% smectite, SHARP WP1.2 Report, 2023, Table 3-4) appropriate properties can be determined.

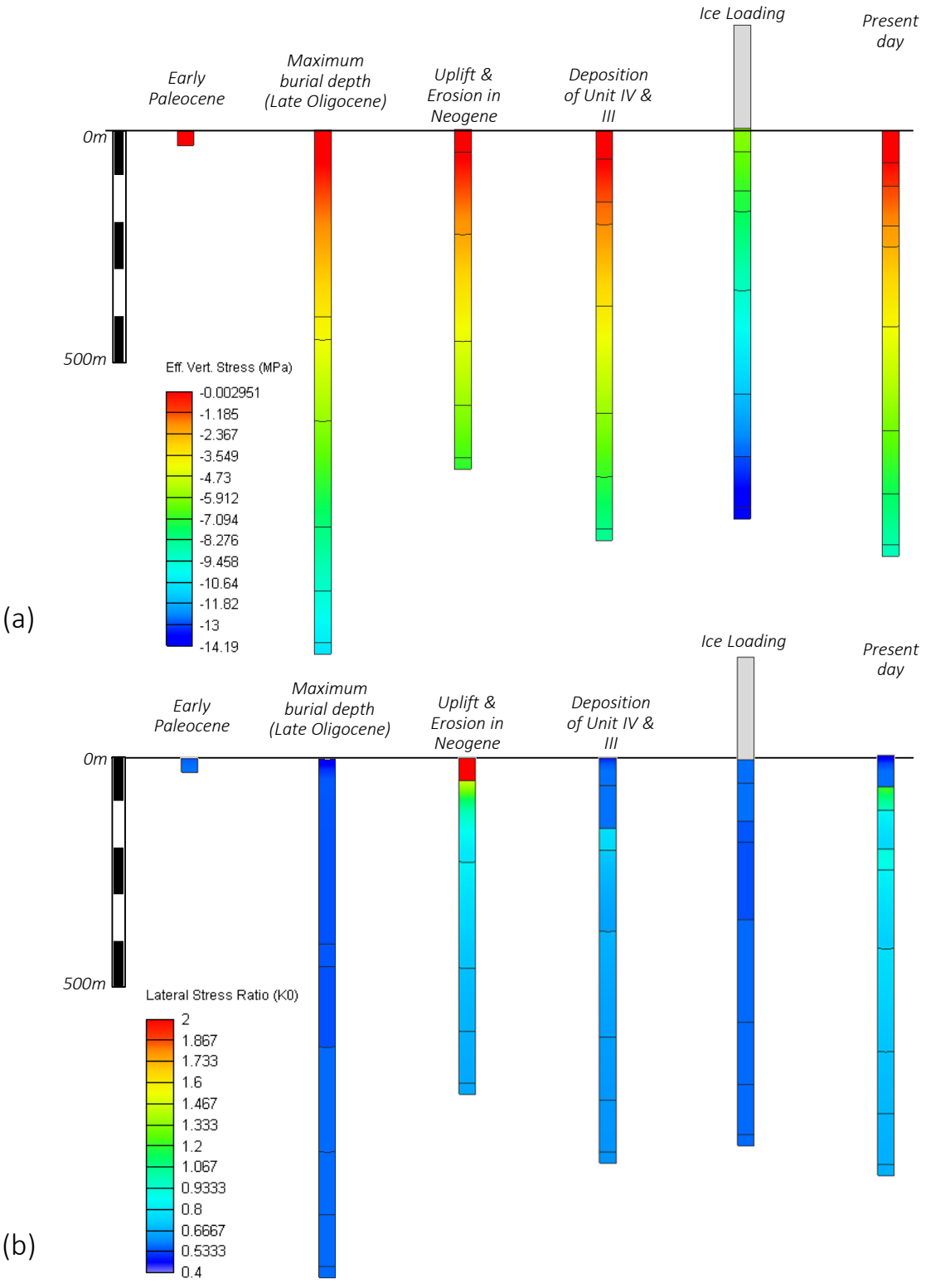

Figure 3-4 Simulated evolution of (a) effective vertical stress and (b) the lateral stress ratio K_0 from Early Paleocene through to present day. Note contour scale maximum is set to 2 – some values locally exceed this value. Ice thickness is demonstrative and not to scale.

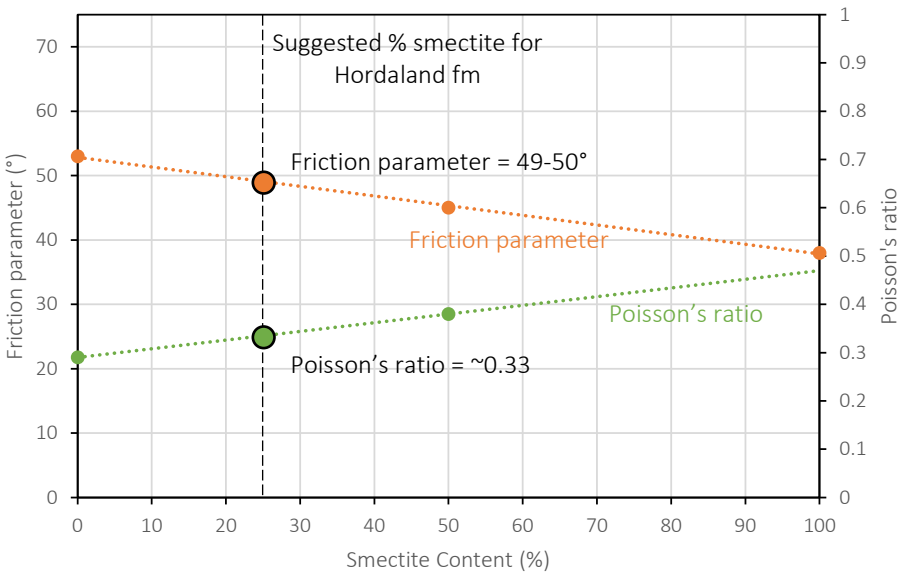

Figure 3-5 Establishing appropriate constitutive parameters for Tertiary age smectite-rich claystones based on characterisation efforts in SHARP task 1.2. Refer to deliverable DV1.2 for more details. Caution: the friction parameter is not the same as Mohr-Coulomb friction angle as it is defined in a specific stress space (q-p'). See DV1.1b report for definition.

The results for Simulation B are shown in Figure 3-6 (blue dashed line). The influence of the modified constitutive inputs is shown to increase the final K_0 within the lower Tertiary and a final value of 0.851 is predicted at the approximate location of the LOP measurement. This agrees quite well with the interpreted value of 0.855 (Grande et al., 2022), and supports that high plasticity clays might be a validate explanation for the anomalous value.

Further simulations have been performed that relax the drained assumption and couple mechanical deformation to porous flow calculations (Thornton & Crook, 2014). The simulations are referred to as Simulations C and D in Figure 3-6 and explore two different porosity-permeability trends. The trends are shown in Figure 3-6(b) which were developed through previous characterisation efforts (SHARP WP1.2 Report, 2023). The intermediate and low permeability trends are adopted for simulations as these appear most representative based on testing of laboratory samples obtained through SHARP work package 3 (SHARP WP3.2 Report, 2023) – these are marked as red triangles on the figure. The trends are applied to the entire Tertiary sequence. The shallow sediments are assigned such that they recover a drained response and the applied glacial loading remains the same – future work may investigate these assumptions in more detail. The predicted K_0 curves are shown in Figure 3-6(a). The intermediate permeability trend predicts a similar trend to the drained base case simulation. Application of the low permeability case results in a more interesting response, and the recovered trend indicates K_0 values that lie closer to the log-based trend that is not corrected for unloading. Assessment of the evolution of pore pressure at the approximate location of the LOP, Figure 3-7(a), from deposition in the early Oligocene through to present day is shown in Figure 3-7(b). As the sediment builds to the maximum burial depth in the early Neogene an overpressure of 1.1MPa is predicted. During the Neogene uplift and erosion the degree of overpressure reduces until a hydrostatic pressure is attained. The nature of this reduction might change with different assumed uplift rates – the model assumes a linear uplift of ~23m/Ma.

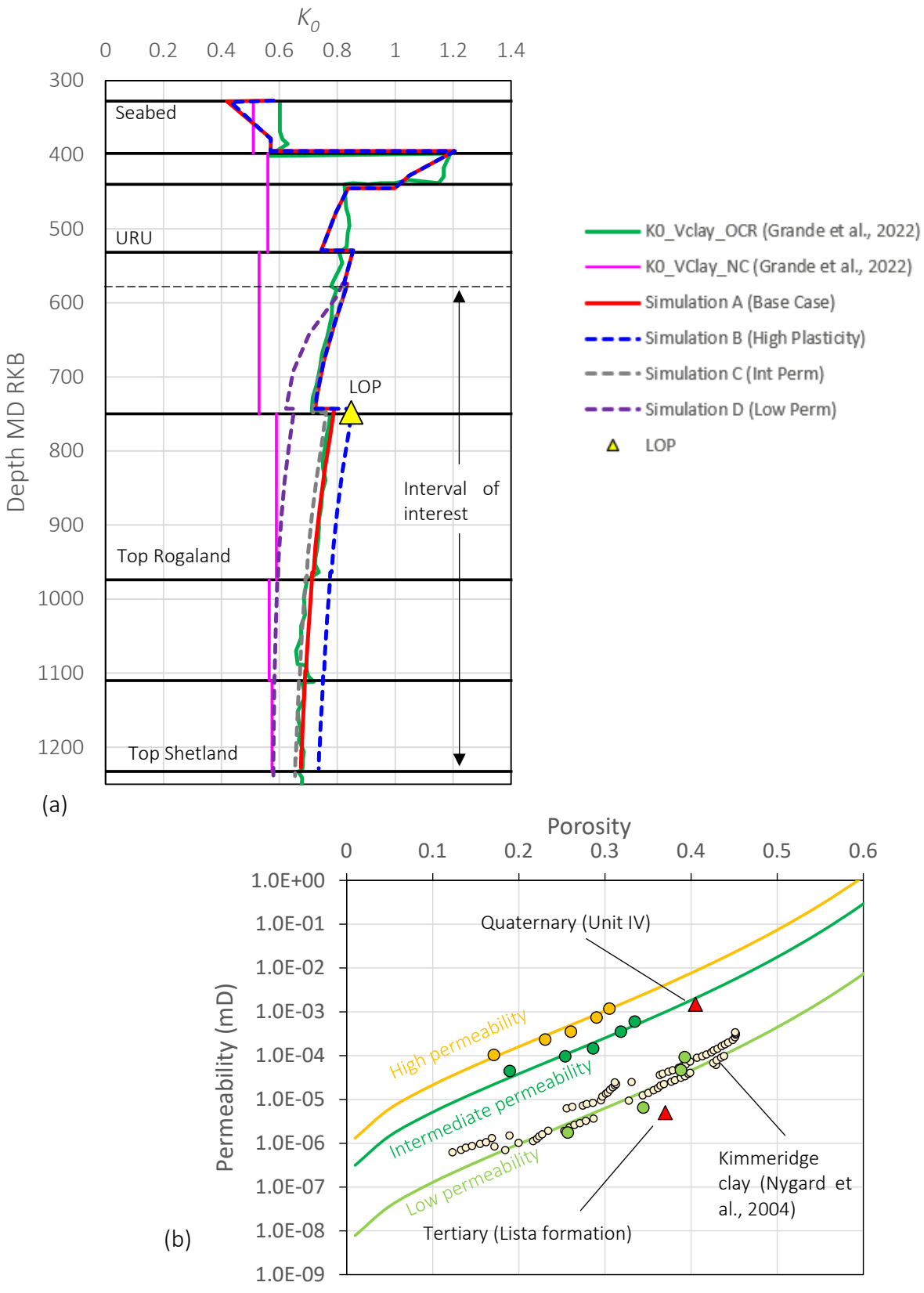

Figure 3-6 (a) Comparison of K_0 variations with depth for Troll East well 31/6-1 under various modelling conditions. (b) Porosity-permeability trends used for fully coupled modelling. Trends have been developed and reported in Task 1.2 based on data from Grande et al., 2013 (filled

circles). Data points supplied through DV3.2 are shown with filled triangles. Note log based K_0 trends are simplified versions of the published data.

The most recent 2Ma is shown in more detail in Figure 3-7(c) and indicates some additional minor overpressure developing during the emplacement of Unit IV and III before significant overpressure development arising during the addition of the glacial load. The overpressure at this point is around 3.55MPa. Importantly, it appears that once the glacier retreats and the load is removed it is possible for an *underpressure* to develop of the order of 1MPa. Underpressure development as a consequence of glaciation has been documented previously – see Wangen et al., 2016) for assessment in the Svalbard area.

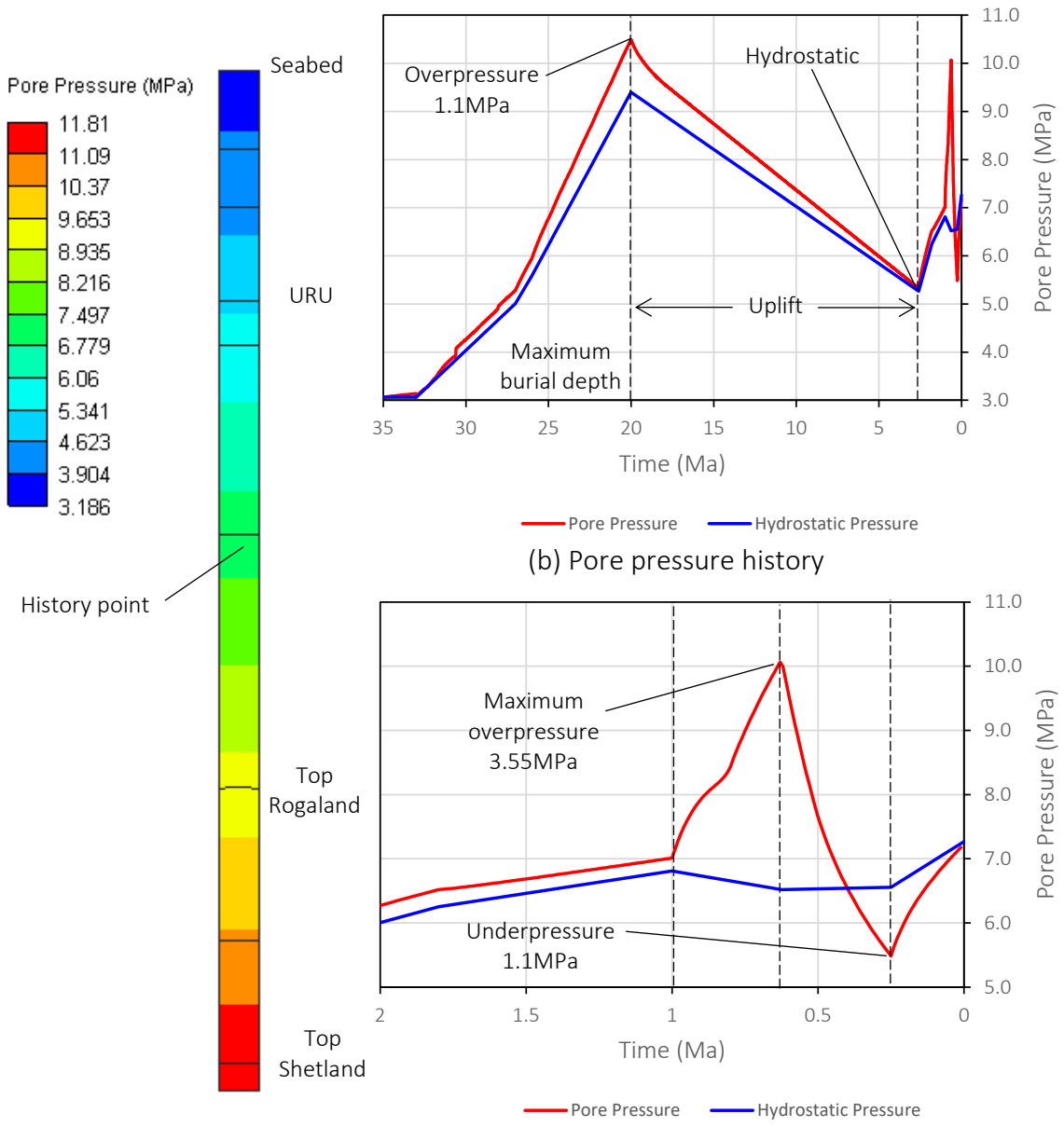

Figure 3-7 Evolution of pore pressure relative to hydrostatic at the approximate location of the leak-off pressure within the Hordaland group (a) Location of pore pressure interrogation point

relative to final (present day) model result (b) Pore pressure history from deposition through to present day (c) Zoom showing pore pressure changes over most recent 2Ma.

As noted by Wangen and co-workers, and supported by the references therein, the reported instances of underpressure globally are almost exclusively associated with glaciation and erosion. At present day pressures close to hydrostatic are predicted. The consequence of underpressure development is to allow for additional compaction (from higher effective stresses) as the glacial load is relaxed, and therefore smaller final values of K_0 are anticipated and indeed observed. Additional glacial load cases have been explored and are shown in Figure 3-8. In Variation 1 (black curve) the load from the glacier is applied more rapidly, resulting in a more rapid initial pore pressure development (arising from increased volume strain rate). The load is then held reflecting a static glacier and excess pore pressure dissipates slightly. The deglaciation is also more rapid and this has an implication in terms of the extent of underpressure. Once Unit I/II is emplaced there is a residual underpressure. A conceptual but perhaps more realistic case is explored in variation 2, where a cyclic variation of loading is included that represents periodic glacial advance and retreat. Loading is ramped up and down over periods of either 50-100ka. This produces a more complex response which is not dissimilar to responses reported by others (e.g. refer to Wangen et al., (2016), and specifically their Figure 4). Approximately hydrostatic conditions are predicted at present day.

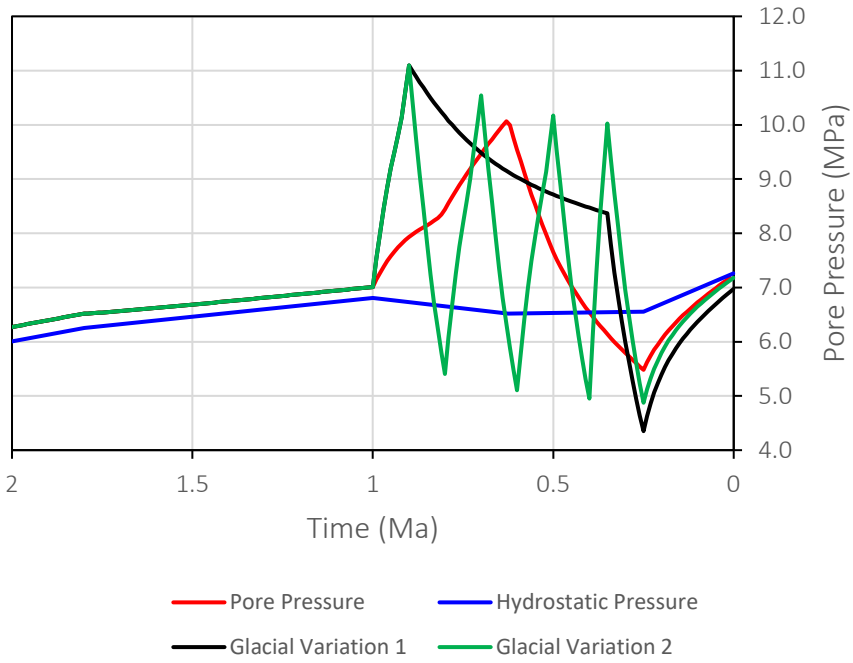

Figure 3-8 Influence of rates of glacial loading and unloading on pore pressure development within the most recent 2Ma.

The implications of modelling results are discussed in the concluding chapters, but the results indicate that simple investigations that integrate sediment composition and constitutive behaviour can help explore uncertainties. In the scenarios explored here featuring realistic stress histories and sediment drainage characteristics it would appear that elevated pore pressures are not predicted and that the anomalous Shmin value is perhaps better explained by high sediment plasticity. However, modelling assumptions and the limitations inherent to the 1D approach should be considered carefully. Ultimately, more extensive investigation is required to better understand pore pressure development as a function of constitutive properties

and stress history, and in particular the effect of geologically recent yet potentially significant loading from glaciers. The results of the models described in this section are summarised in Table 3-1. For reference the estimated LOP at 748mKB is 1.46g/cc giving approximately 10.71MPa and K_0 is equal to 0.855 (calculated assuming hydrostatic pressure).

Sim. Ref	Simulation Summary	K_0 @ LOP depth	Approx. Shmin @ LOP depth (MPa)**	Over-pressure (MPa)
A	Drained conditions (base case).	0.788	10.51 (-0.2)	0
B	Drained conditions. High plasticity clays applied to early Tertiary sediments.	0.851	10.77 (+0.06)	0
C	Coupled hydro-mechanical modelling. Intermediate range porosity-permeability curve applied to Tertiary sediments.	0.761	10.54 (-0.17)	0.13
D*	Coupled hydro-mechanical modelling. Lower bound porosity-permeability curve applied to Tertiary sediments.	0.651	9.96 (-0.75)	-0.04

*Table 3-1 Summary of modelling variations. * Values for D based on initial glacial loading curve ** Values in brackets show value relative to Shmin derived from LOP measurement.*

3.3.2 Extending Modelling to Incorporate Deeper Reservoirs and Sealing Units

The primary storage target at the nearby Smeaheia site is the Sognefjord formation which is sealed by the overlying Draupne and Heather formations. There is also potential for storage in the deeper sandstones of the Cook formation which is sealed by the Drake formation. As such there is value in extending the developed models to greater depths to include these units and incorporate elements of the work from chapter 2 – see Figure 3-9. The most significant change is the hardening trends applied to the various layers to better approximate the bulk density trend.

The simulations start from the Early Jurassic (Toarcian) with the deposition of the Drake formation through to present day. An interrogation of K_0 trend is shown in Figure 3-10(a) for two different set of inputs. The base case follows the approximate clay fraction reported by Grande et al., (2022) with the exception of the Drake formation. Note that the trend shown is a smoothed and simplified version of the curves reported by Grande et al., 2022. Below the Heather formation for instance there is a transition to a more sand dominated regime which shows significant variation in K_0 based on log data resulting from layering of sediments with variable clay contents (sandy versus shaly/silty).

The output of the numerical simulation again agrees quite well with the simplified log-based trend. The circled regions focus on the Drake formation, which shows slightly lower K_0 values as it has reached temperatures sufficient to start chemically compacting. A single characterisation has been assumed for the Drake formation for reasons of simplicity and the implications of this are discussed later. Examining the density trend in (b) shows that there is generally good agreement with the average density trend, however there is some mismatch in the bulk density in the Drake formation. Porosity changes are not significant enough to satisfactorily approximate the observed bulk density, and two points are worth considering here:

- The diagenetic law is very simple and although encouraging correlations were observed in earlier chapters it is highly unlikely that it will provide robust

predictions across wells where burial/thermal histories and sediment composition can vary widely.

- The simplicity of the diagenetic model is an issue particularly during uplift as one component of the model relies on increasing temperatures. When the material becomes uplifted the rate reduces, as expected, but likely too aggressively resulting in less significant porosity changes. This would be especially significant during the early stages of uplift.

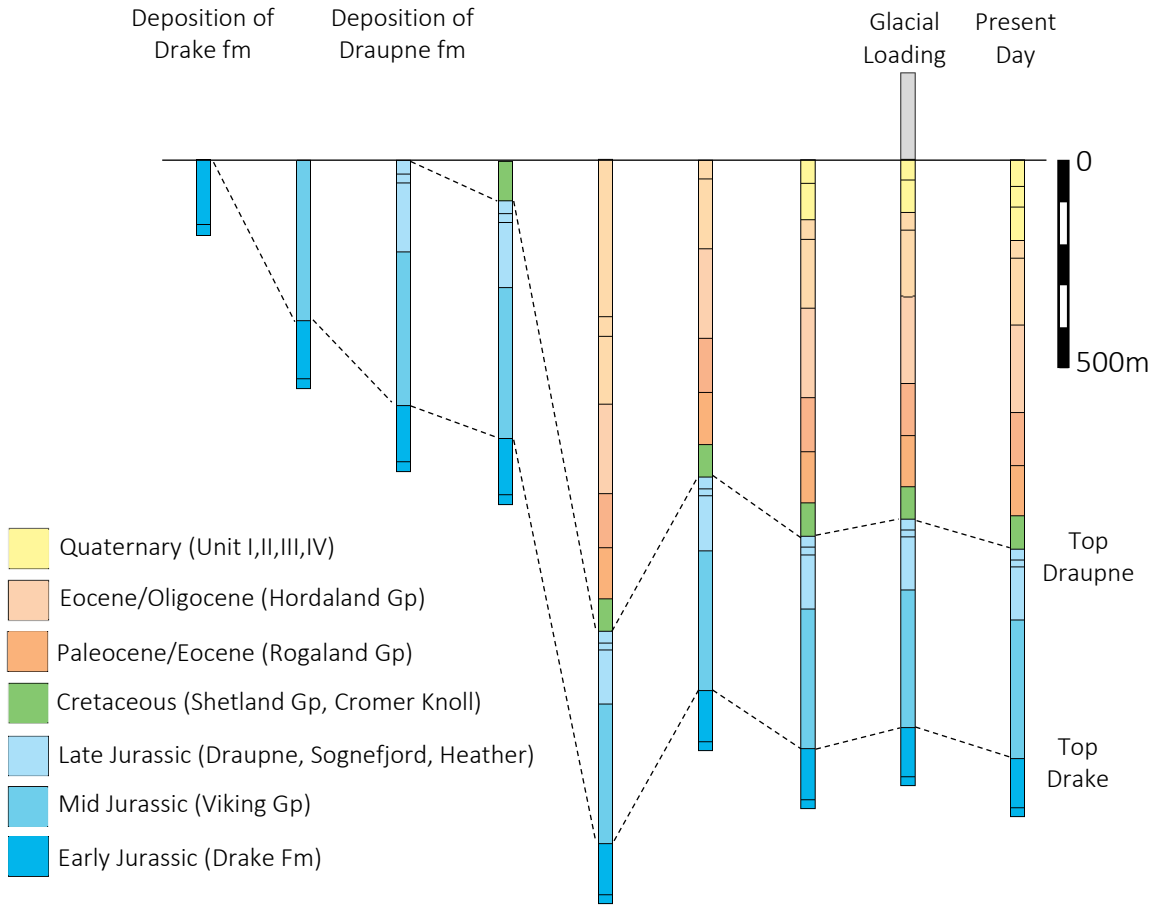

Figure 3-9 Configuration for extended simulations of the Troll 31/6-1 well including Jurassic and Cretaceous age sediments.

To counter this an additional simulation has been performed which permits a modified temperature range for diagenesis within the Drake formation, reducing from the base case simulation range of 60-130°C to 50-120°C. This provides an improved density correlation and, as the reaction has been progressing over a longer duration, a reduced final K_0 value is predicted. The modelled range of K_0 values for the Drake formation is between 0.52 and 0.51 which agrees reasonably with the value of 0.54 reported by Grande et al., (2022). However, there is some uncertainty associated with this value and it is quite probable that it in fact reflects stress conditions in the underlying Cook formation. Further changes introduced in the variation model are seen in the shallower sections – the high plasticity assumption in the lower Tertiary is retained and also the Draupne formation characterisation shown in Figure 2-5 is incorporated. Integrating these changes shows better correlation with LOP measurements at these depths. The LOP within the Draupne is significant as it is a regional seal and the

difference between the K_0 predicted in the two models is around 0.22 which translates to around 2MPa. This is a reasonably significant difference that might have implications for assessments of the risk of caprock fracturing for instance.

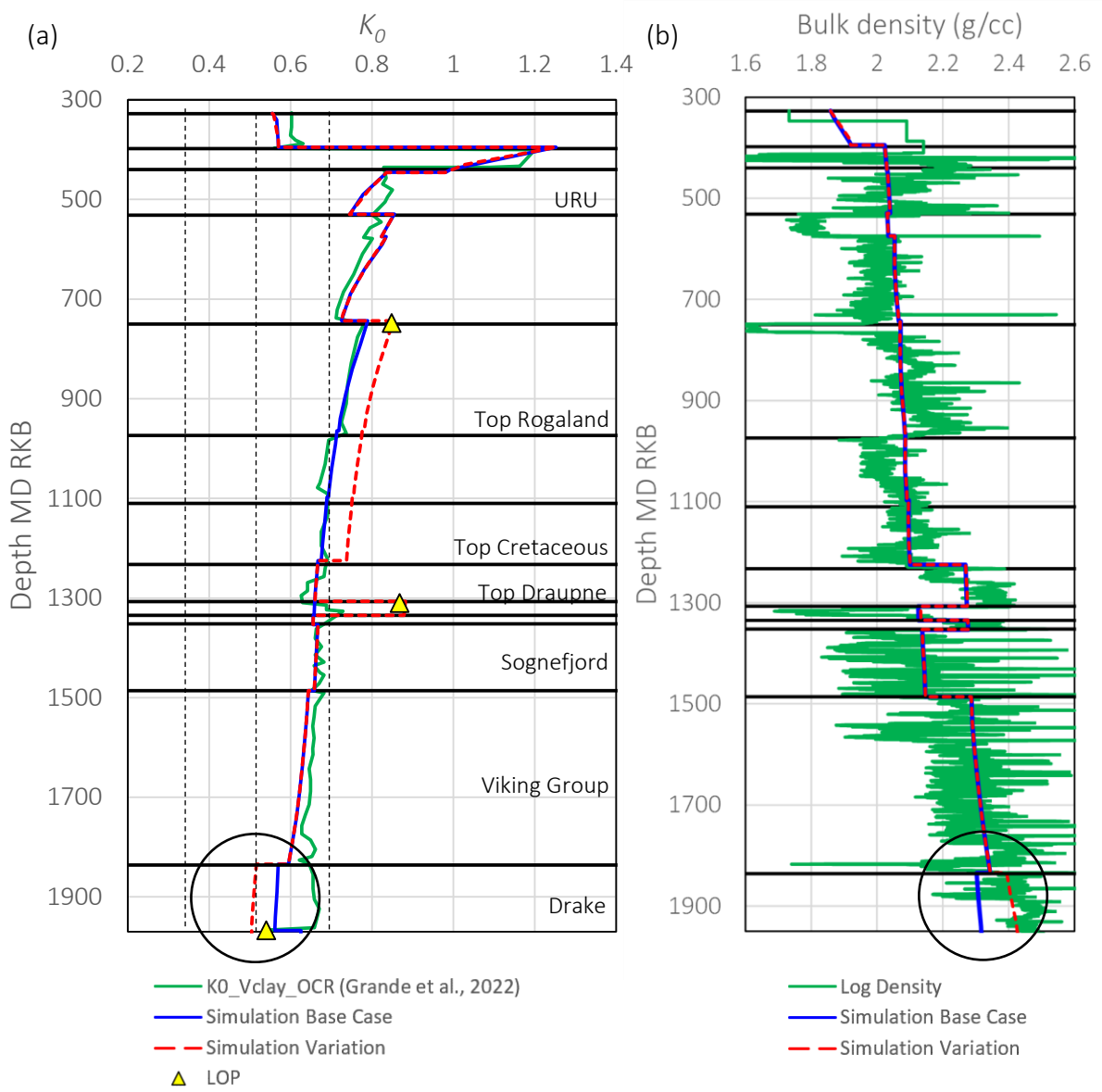

Figure 3-10 Interrogation of Troll 31/6-1 well model at present day configuration showing (a) K_0 (b) bulk density. Note log based K_0 trends are simplified versions of the published data.

The evolution of K_0 is shown in Figure 3-11. The contour scales is set to correspond to suggested ranges reported in DV1.2 – with K_0 typically suggested to lie in the range 0.6+/-0.2. Warmer and cooler colours indicate values of K_0 greater and less than the mid-range value respectively. The results again highlight the significant changes that occur from the more recent stress drivers (uplift, erosion). One key observation is that at the maximum burial depth, inspite of lithological variability, the range is much narrow generally 0.6+/-0.06 and so in areas experiencing minor uplift and limited glacial loading the general mid-range value is quite representative. The significant change from uplift and glacial loading in the Horda area result in a broader range, particularly in the shallow depths. The obvious change to cooler colours in the Drake formation identifies the contribution of deeper diagenetic processes.

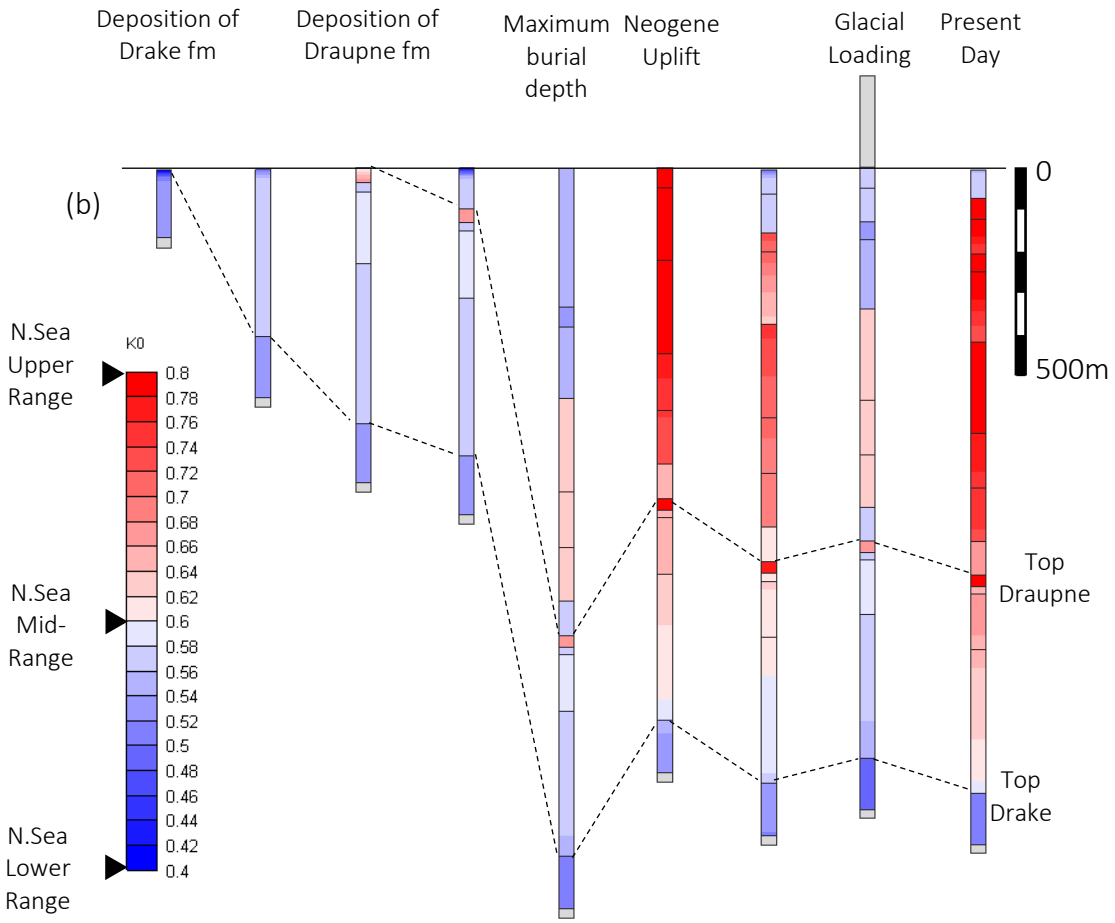

Figure 3-11 Evolution of K_0 at the Troll 31/6-1 well including Jurassic and Cretaceous age sediments. Note that contour scale has maximum range set to 0.8 but locally values exceed this e.g. within the heavily overconsolidated quaternary units.

3.4 Summary

Modelling within this chapter has focused on a specific, data-rich well in the Horda Platform area – Troll 31/6-1. The evolutionary modelling framework based on an adaptive finite element approach is able to explicitly represent the key geological processes identified in earlier stages of the SHARP project, namely deposition, erosion/uplift, and glacial loading. Encouragingly when consistent inputs and assumptions are applied the modelling output predicts similar trends for K_0. This is not unexpected as some of the same source datasets are used, albeit in different ways. Relationships between the amount of clay and key constitutive model parameters allows for adjustment depending on the lithological composition of layers, again showing favourable agreement with the log-based methods. Characterization efforts in WP1.2 also have allowed for adjustments based on smectite content. Additional datasets exploring sediment composition in more detail would permit for these relationships to be used more confidently. An advantage of the modelling framework is that it can move beyond some of the limitations of the log-based approach. Notably the assumption of a drained response can be relaxed through coupled simulation, and the work on diagenesis from earlier chapters allows for some assessment beyond the mechanical compaction domain. The implications of these factors for subsurface storage are discussed in the following chapter.

4 Discussion

4.1 Impact of Burial Diagenesis

The analyses undertaken in Chapter 2 investigated possible influences of coupling a simple diagenetic law to the characterisations developed in WP1.2. Alterations to fundamental mechanical properties as a function of diagenesis were introduced and the effect on K_0 was explored in single element simulations under basic stress and temperature loading. The key observations were that:

- When diagenesis is considered the observed effect is *to reduce K_0 during burial*. The extent of this reduction was dependent on key assumptions such as the degree of overconsolidation arising from diagenesis or if the influence of changing mineralogical composition (e.g. smectite to illite) on fundamental properties is considered.
- Through lowering K_0 under burial the material is preconditioned to be less sensitive to unloading for a given Poisson's ratio. This was discussed in DV1.2.
- Should the diagenetic reaction introduce significant anisotropy, particularly at a late stage, this was demonstrated through a simplified approach to lead to scenarios in which *K_0 can decrease during unloading*. As significant anisotropy in shales is often attributed to deep burial and extensive diagenetic alteration this could be an important factor to consider, and explain the different responses observed in shallow (mechanical compaction only) versus deep (additional chemical affect) sediments.
- More experimental work to explore and confirm some of the proposed mechanisms would be invaluable in future. It is also important to note that it is often challenging to determine Poisson's ratio in experiments, though the deformation modelling has identified this as an important parameter in stress evaluation.

Based on these observations the following suggestions are offered for stress determination workflows:

- Unloading correction for shales in log-based stress determination workflows buried beyond ~60°C should be considered carefully. It might be prudent to neglect the OCR correction altogether as modelling and experimentation suggest altered shales in particular are less sensitive to unloading. Possible reasons for this behaviour have been outlined.
- If it is possible through available logging methods to develop an appreciation for the degree of anisotropy then potentially specific corrections to K_0 could be made based on the inferred amount of stress relief through unloading. Additionally, if logs can offer insights into the degree of diagenetic alteration and cementation (through bulk density or porosity) it might be possible to correlate these to K_0 instead of clay fraction – see (Grande et al., 2011) for example.
- The uncertainties in the precise nature and influence of diagenetic processes on stress is reflected by challenges accurately representing them in numerical simulations. Such uncertainties can therefore result in a wide-range of potential deformation histories and quite different final stress predictions. The predictions made still fall within the North Sea regional upper-lower bounds (see Figure 2-7) and these therefore provide useful constraint in the absence of detailed local knowledge/data. Given the probable variability in properties and nature of the sediments both vertically and laterally, effort

should be accorded to assessing the risk via probabilistic methods – see output of SHARP WP5.

4.2 Stress History, Lithology Variation, and Uncertainties

4.2.1 Assessment of Secondary Seals

Models incorporating stress history were explored in Chapter 3, with a focus on Troll East well 31/6-1. As noted earlier the modelling framework showed good agreement with log-based workflows developed in DV1.2, and procedures for adjusting constitutive parameters according to clay content were introduced (Figure 3-2) – additional data will help to confirm the suitability of the trends and allow them to be used more widely across the North Sea.

The modelling framework offered the possibility to study pore pressure development through coupled models. The motivation for exploring coupled models was primarily to better understand the possible source of the high LOP in the Tertiary at Troll. Two reasons were hypothesised (a) local overpressure leading to elevated Shmin, or (b) the presence of plastic clays within this interval leading to elevated K_0 and high Shmin. Integrating realistic permeabilities for the Tertiary revealed that the uplift may lead to dissipation of any overpressure developed before the Neogene. Furthermore, whilst the influence of rapid glacial advance was demonstrated to lead to quite significant overpressure, subtle underpressures were predicted at present day due to rapid glacial retreat. The development of underpressure as a consequence of glacial advance/retreat has been explored elsewhere, and further checking and analysis in this direction would be worthwhile in future. Nevertheless, the modelling presented would suggest hydrostatic pressures are more likely and this is compatible with operational experience in the Horda Platform (Thompson et al., 2022; Equinor pers. comm). This suggests the elevated Shmin value is not associated with overpressured sediments.

To explore the significance of plastic clays relationships between the key constitutive parameters (friction angle, Poisson's ratio) and smectite content were developed using characterisations from WP1.2 (Figure 3-5). When these were introduced it was found that values of K_0 were obtained that agreed with the LOP quite well, suggesting this to be a valid hypothesis. Supporting evidence to further substantiate this mechanism comes in two forms:

- The density trend in the Tertiary is quite steep and is well fitted by the hardening properties derived from smectite rich synthetic material. Smectite rich sediments can retain higher porosities and by extension low velocities.
- The lower Tertiary age sediments across the Horda platform host a polygonal fault system; Figure 1-2, Figure 4-1. This particular class of intraformational fault is closely associated with high plasticity sediments that have low residual friction angles (Cartwright & Dewhurst, 1998; Dewhurst et al., 1999; Goulty, 2001, 2008; King et al., 2022). Their presence is therefore suggestive of highly plastic clays within this interval.

These observations have the following consequences for shallower secondary seals:

- Stress relief from uplift and glaciation lead to elevated horizontal stresses which may exceed 1 near surface. Fractures propagating towards the surface would turn normal to the minimum stress (vertically) and would be less likely to reach the surface.
- Overpressuring was not predicted in the simulations at present day, and highly plastic clays was suggested to be a better candidate for explaining elevated Shmin. Collectively this means higher effective normal stresses acting on faults within these intervals, and in general through much of the overburden.

As suggested in DV1.2 report, regional trends (Thompson, Andrews, Reitan, et al., 2022; Thompson, Andrews, Wu, et al., 2022) will be invaluable at early stages of site appraisal for determining expectations. Anomalous values that do not conform to regional expectations can be checked against known sediment composition/characteristics and, importantly, stress history to develop a better local understanding of *in situ* stress. Following this procedure for the Troll well allowed for good approximation to known data points and stress conditions, revealing more favourable shallow stress conditions in terms of fault reactivation.

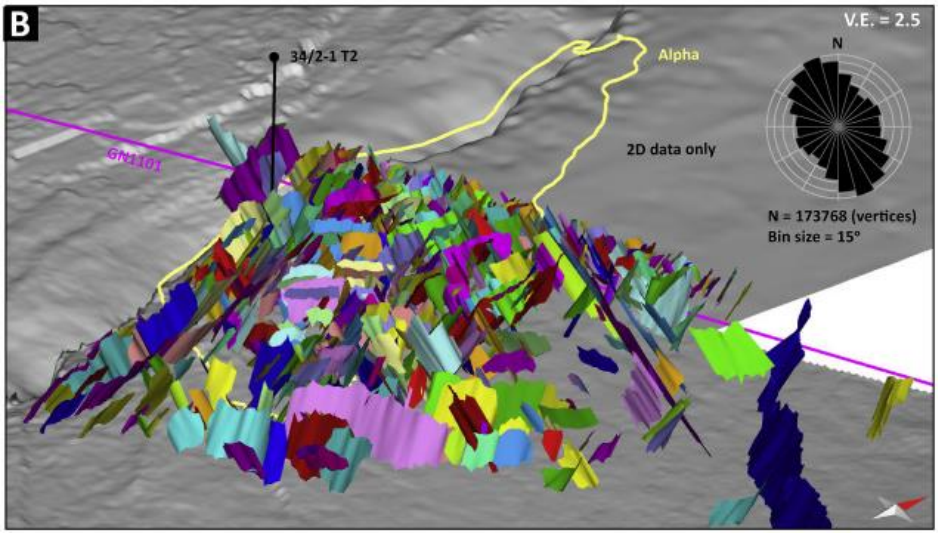

Figure 4-1 Polygonal faults within the overburden (Eocene and Oligocene) in the Smeaheia area (Mulrooney et al., 2020).

4.2.2 Assessment of Deeper Units Including Primary Seals

Subsequent models at Troll extended the depth range to permit consideration of key intervals such as the Draupne and Drake formations, which overlie the regional targeted storage units. The Draupne formation likely hasn't been heavily diagenetically modified at this location as the burial is shallower than at Smeaheia. Integrating best estimates for key properties (based on K_0 testing on Draupne material from Troll and friction angle from samples in the Ling Depression) resulted in a final stress prediction that agreed well with the LOP measurement. As noted the LOP is suggestive of an Shmin much higher than the regional value which again would seem advantageous from the point of view of maintaining caprock integrity, and underscores the potential for developing better stress estimates through deeper understanding of stress history and sediment properties.

The Drake formation likely has started to undergo some diagenetic modification and the result of this was evident in the stress profiles, with cooler values evident at depth. Further models should seek to extend the depth further to confirm the trends suggested in DV1.2.

4.2.3 Limitations and Uncertainties

It is important to emphasise the limitations and uncertainties associated with the modelling work. Importantly, many of the calibration points used are from LOP data, and are of lower quality in terms of stress calibration, and even higher quality XLOT data is open to interpretation. The modelling work suffers from some limitations, notable the requirement to homogenise sedimentary packages to make modelling tractable means that key units that may act as e.g. stress barriers are excluded, and the uniaxial/1D modelling means limited capability

to accommodate regional tectonics or lateral flow. Both these aspects can be addressed in future work. Incorporating the more realistic representation of stratigraphy should focus on the key sequences – for example the Drake formation is represented as a single unit with unique properties. It would be more appropriate to break this down into the various subgroups (Thompson et al., 2022) as these have distinct compositions and there is direct evidence of stress variability. Accounting for diagenesis is challenging and although some models have successfully correlated to in situ observations and are partially constrained by experimental data, regionally there likely exists significant variability in the nature, timing and resulting impact of diagenetic processes. It is also important to recognise the uncertainty in the *in situ* measurements; LOP have lower confidence compared to XLOT, and there is often assumptions or uncertainties associated with the derived stress values. Ultimately, there will exist uncertainty in the *in situ* stresses, both measured and simulated, particularly where the sediment behaviour becomes more challenging to replicate (experimentally and numerically). Probabilistic methods (Task 5.1) are best suited to exploring the uncertainties.

4.3 Extension to Proposed Storage Sites

4.3.1 Smeaheia Alpha 32/4-1

Proposed storage at the Smeaheia Alpha site is a short distance east from Troll. Preliminary investigations of the response at the Alpha site have been undertaken and are summarised in Figure 4-2. The analysis includes Late Jurassic and younger sediments (deepest sediment simulated is Draupne formation). The modelling process is repeated and representative constitutive inputs are sought based on simplified clay fractions for the bulk layers incorporated in the model – Figure 4-2(a). The Shetland and Rogaland groups are subdivided because of the more variable clay content. Two simulations are performed denoted 32/4-1 v1 and 32/4-1 v2, with the only difference being the characterisation applied to the Draupne formation. One characterisation (v2) is the same as applied to the Troll model, and the other is identical save for a larger Poisson's ratio value (0.29 versus 0.2). The final predicted K_0 for the simulations is shown in Figure 4-2(b), the contours again show elevated K_0 relative to the mid-range North Sea value of 0.6. The only distinction between the models is the response in the Draupne formation, where the v1 simulation shows smaller K_0 values due to increased Poisson's ratio. Comparison to a simplified K_0 trend derived from Grande et al., 2022 is provided in Figure 4-2(c) and shows reasonable agreement, although there is some mismatch in the lower Rogaland unit.

Stress data available for this well includes LOP measurements in the Lista and Draupne formations (CO2datashare Smeaheia dataset) – see Table 4-1. A key assumption is that the density profiles can be translated directly to this well from the Troll model, and as a complete density log for well 32/4-1 is not available the validity of this assumption cannot be assessed. This also makes it difficult to calculate the equivalent value of K_0 and therefore these calibration points are not shown on the plots. As means of comparison the model total minimum stress is compared to the LOP value directly in Table 4-1.

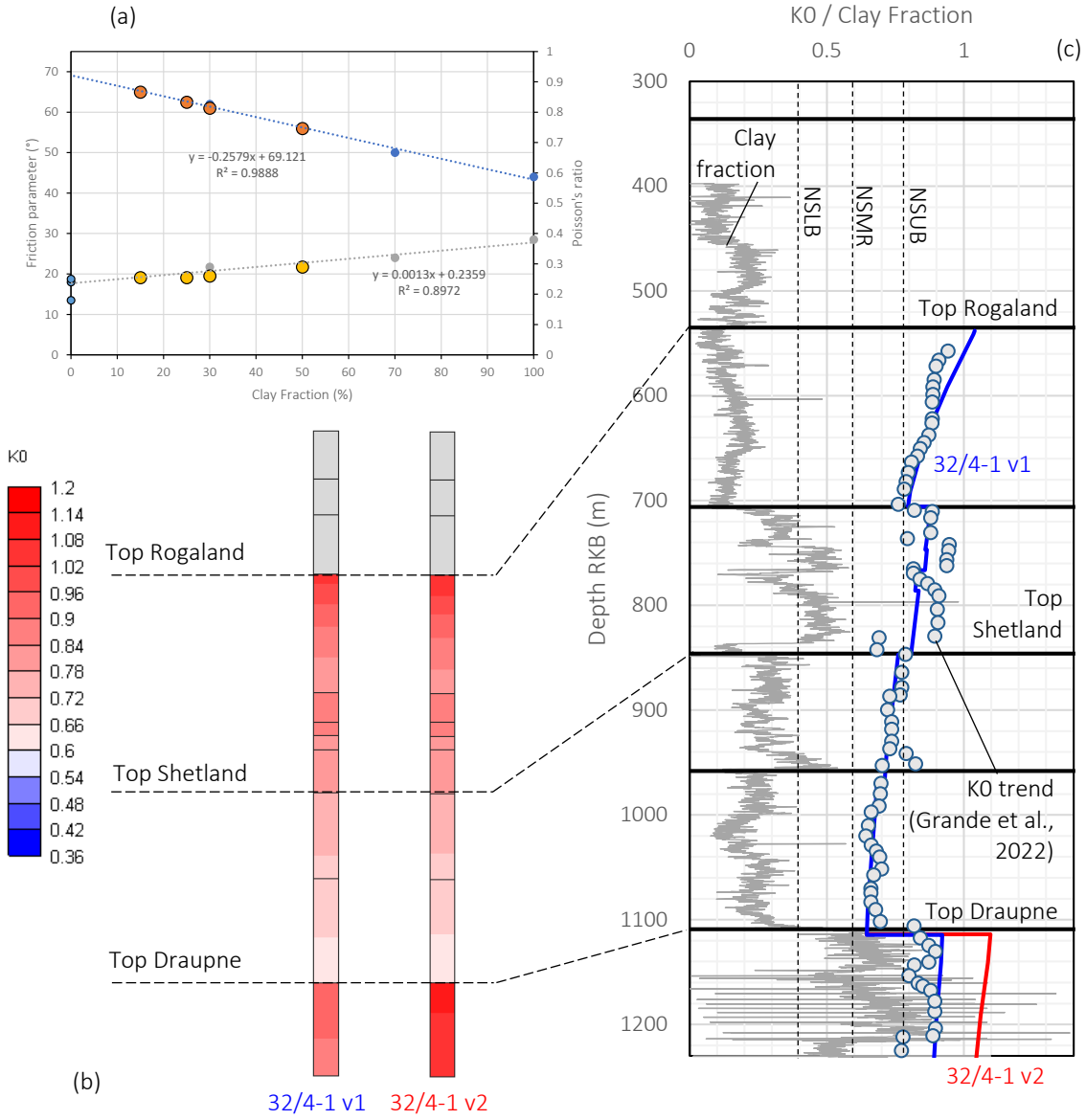

Figure 4-2 Preliminary translation of modelling workflow to well 32/4-1 Smeaheia Alpha. Note log based K_0 trends are simplified versions of the published data (a) selection of constitutive parameters based on representative clay fractions (b) (c) Predicted stresses compared to average trend reported by Grande et al., 2022. NSLB – North Sea Lower Bound K0, NSMR – North Sea Mid-Range K0, NSUB – North Sea Upper Bound K0.

Formation	Approximate Test Depth (mKB)	Leak-Off Pressure (MPa)	Model Shmin (MPa)	Difference (%)
Lista	708	11.25	10.12	-11.12
Draupne	1137	18.18	20.23	+10.11

Table 4-1 Comparison of observed (LOP) and simulated Shmin values in Tertiary (Lista) and Draupne formation for well 32/4-1 Smeaheia Alpha. Results are based on simulation 32/4-1 v1.

The value in the Lista formation is smaller than the LOP value by about 10% and conversely the value is around 10% larger than the LOP value in the Draupne formation. Several points are worth considering here:

- There is uncertainty in the density profile and by extension the overburden stress which could be a source of error.
- The LOP in the Lista formation is again quite high. High plasticity clays could also be present here and lead to elevated K_0.
- The Draupne formation has been buried to depths where diagenesis may be active. As commented by Grande et al., (2022) this may have resulted in more limited change in K_0 on unloading.
- Again it is emphasized that LOP is a less accurate measurement of *in situ* stress. XLOT may provide a K_0 value 0.06-0.1 lower than LOP (Grande et al., 2022) and so the modelled value in the Tertiary for instance may be representative.

Further simulations to address the above points in more detail is planned.

4.3.2 Incorporating Insights into 3D Geomechanical Modelling Workflows

Elevated minimum stresses in the shallow are indicated by LOP tests in the Horda Platform area and predicted reasonably accurately in both log-based workflows and forward geomechanical models when the stress history and sediment composition are integrated into the characterisation approach. An open question to address is just how significant this might be in terms of operational risks/opportunities and monitoring requirements during storage. Specific attention in the SHARP project is being accorded to the stability of the Vette fault.

Understanding the influence of stress history in this regard is best tackled via integration of some of the techniques into the stress initialisation process for 3D geomechanical models. This would then permit exploration of the consequence of proposed injection scenarios on stability of the Vette fault. The preliminary stages of this workflow have been developed (Figure 4-3) and will be developed further in Task 1.4/1.5. The stress initialisation workflow takes the following form:

1. Map Vclay to finite element mesh. This may be spatially varying (from inversion) or averaged per layer/formation.
2. Establish overburden stress, S_v, using spatial variation (from inversion), averaged layer densities, or representative North Sea density profiles.
3. Establish pore pressure profile, P_p – hydrostatic pressures can be assumed for the area based on this report and operational experience.
4. Map uplift distribution (SHARP WP1.2 Report, 2023) to finite element mesh – see Figure 4-3(a). Using overburden stress and assumed density for removed material establish OCR – see Figure 4-3(b).
5. Use Eq. 3 or 4 (with and without OCR correction) to establish initial K_0 value per finite element ((Grande et al., 2022):

$$K_o = 0.0034V_{clay} + 0.3681 \quad \textit{Eq. 3}$$

$$K_o = (0.0034V_{clay} + 0.3681) \cdot OCR^{0.47} \quad \textit{Eq. 4}$$

6. Set horizontal stresses using combinations of the above i.e. S_v, P_p, K_0. Set maximum horizontal stress azimuth and stress anisotropy according to regional experience .
7. Allow stresses to equilibrate. Assess initial stresses on key faults e.g. Vette.

8. Incorporate pore pressure changes via injection loading histories and assess fault stability in scenarios with/without stress history correction.

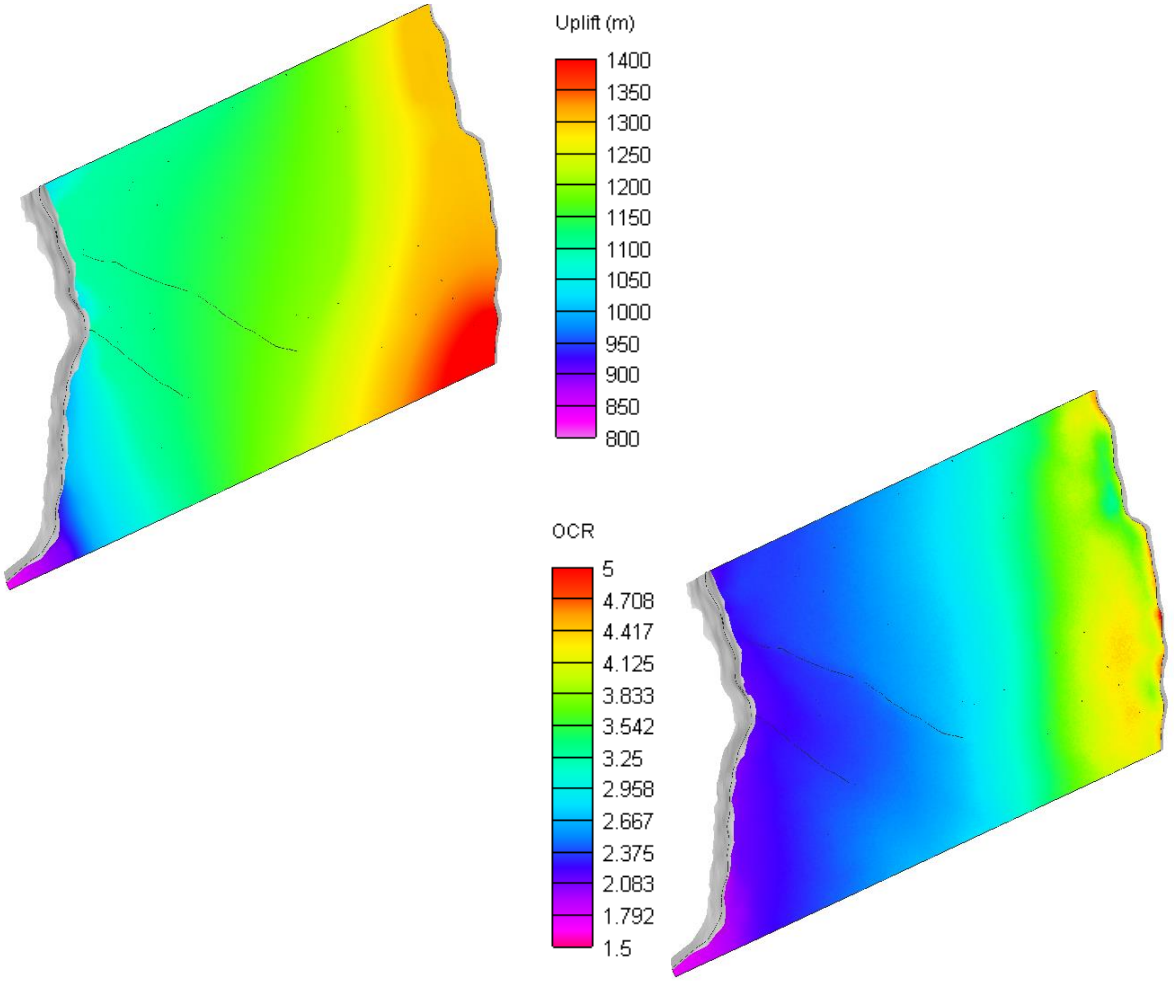

Figure 4-3 Development of procedures for integration of stress history into initialisation process (a) Uplift map developed in SHARP Task 1.2 mapped onto the finite element mesh (b) Predicted overconsolidation ratio. Both images are shown at level of Top Druapne shale from prototype 3D Smeaheia model.

5 Conclusions & Further Work

5.1 Conclusions

This report has focused on exploring the significance of stress history and sediment composition on *in situ* stresses. Simulations that address sediment mineralogy through constitutive modelling and integrate constraints on stress history (uplift, glacial load) have been performed. Encouragingly simulations provide outputs that are consistent with log-based stress characterisation workflows developed under the SHARP project. The simulations have been used to explore the significance of processes that are not accounted for through these workflows, namely overpressuring and burial diagenesis. Simulations focusing on the Troll East 31/6-1 well have shown how high, anomalous stress measurements may be explained through consideration of the stress history and sediment mineralogy.

A key observation is that because of the complexity and variability of processes such as diagenesis even when they are accounted for the in the modelling process there is still significant uncertainty in the stress predictions. Nevertheless the modelling predictions mostly fell within the bounds established in previous works based on assimilation of a large quantity of *in situ* stress measurements. These trends are therefore extremely valuable and may be used in the absence of detailed local knowledge. The variability and uncertainty in variables such as the minimum stress should be tackled via probabilistic approaches and specific work packages within the SHARP project are established to address this.

5.2 Further Work

The work documented here may be developed in a number of directions in future. Some primary areas for focus are:

- Additional investigation into diagenesis in terms of fabric and influence on stress path.
- Integration of the modelling insights into 3D geomechanical modelling workflows is a critical next step. These models can address open questions regarding the significance of stress history in terms of operational risks.
- Focus for modelling has been specifically in the Northern North Sea. Application of modelling techniques for mineralogy and stress history correction for other sites across the North Sea. Proposed storage sites in the Southern North Sea such as Endurance feature older rocks and also the presence of evaporites, which may add additional complexities.

6 References

Andrews, J. S., & de Lesquen, C. (2019, June 23). Stress Determination from Logs. Why the Simple Uniaxial Strain Model is Physically Flawed but Still Gives Relatively Good Matches to High Quality Stress Measurements Performed on Several Fields Offshore Norway. *Proceedings of the 53rd U.S. Rock Mechanics/Geomechanics Symposium, New York City, New York*.

Bjorlykke, K., & Hoeg, K. (1997). Effects of burial diagenesis on stresses, compaction and fluid flow in sedimentary basins. *Marine and Petroleum Geology*, *14*(3), 267–276.

Cartwright, J. A., & Dewhurst, D. N. (1998). Layer-bound compaction faults in fine-grained sediments. *Geological Society of America Bulletin*, *110*(10), 1242–1257.

Charpentier, A. D., Worden, R. H., Dillon B', C. G., & Aplin, A. C. (2003). Fabric development and the smectite to illite transition in Gulf of Mexico mudstones: an image analysis approach. In *Journal of Geochemical Exploration* (Vol. 78). www.sciencedirect.com

Crook, A. J. L., Owen, D. R. J., Willson, S., & Yu, J. (2006). Benchmarks for the evolution of shear localisation with large relative sliding in frictional materials. *Computer Methods in Applied Mechanics and Engineering*, *195*(37–40), 4991–5010.

Crook, A. J. L., Willson, S., Yu, J., & Owen, D. (2006). Predictive modelling of structure evolution in sandbox experiments. *Journal of Structural Geology*, *28*(5), 729–744.

Day-Stirrat, R. J., McDonnell, A., & Wood, L. J. (2010). Diagenetic and Seismic concerns associated with interpretation of deeply buried "mobile shales." *AAPG Memoir*, *93*, 5–27. https://doi.org/10.1306/13231306M93730

Dewhurst, D. N., Cartwright, J. A., & Lonergan, L. (1999). The development of polygonal fault systems by syneresis of colloidal sediments. *Marine and Petroleum Geology*, *16*(8), 793–810.

Ewy, R., Dirkzwager, J., & Bovberg, C. (2020). Claystone porosity and mechanical behavior vs. geologic burial stress. *Marine and Petroleum Geology*, *121*. https://doi.org/10.1016/j.marpetgeo.2020.104563

Goulty, N. R. (2001). Mechanics of layer-bound polygonal faulting in fine-grained sediments. *Journal of the Geological Society*, *159*(1991), 239–246.

Goulty, N. R. (2008). Geomechanics of polygonal fault systems: a review. *Petroleum Geoscience*, *14*(4), 389–397.

Grande, L., Mondol, H., Skurtveit, E., & Thompson, N. (2022). *Stress estimation from clay content and mineralogy-Eos well in the Aurora CO 2 storage site, offshore Norway*. https://ssrn.com/abstract=4286343

Grande, L., & Mondol, N. H. (2013). Geomechanical, hydraulic and seismic properties of unconsolidated sediments and their applications to shallow reservoirs. *47th US Rock Mechanics/Geomechanics Symposium, San Francisco, CA, USA*, 1–10.

Grande, L., Mondol, N. H., & Berre, T. (2011). Horizontal Stress Development in Fine-grained Seimdents and Mudstones during Compaction and Uplift. *73rd EAGE Conference & Exhibition Incorporating SPE EUROPEC, Vienna, Austria*, 1–5.

Griffiths, L., Thompson, N., Smith, H., Grande, L., & Skurtveit, E. (2023). Rock mechanical testing of core from Eos CCS validation well. *Proceedings of TCCS 12*.

Jalali, R. (2022). *Consolidation and stress history in shallow sediments in the northern North Sea*. NTNU.

Johnson, J. R. (2022). *Integrated analysis of kerogen maturation and microfracture dynamics in organic-rich shales*.

King, J. J., Roberts, D. T., Cartwright, J. A., & Levell, B. K. (2022). Numerical modelling of the growth of polygonal fault systems. *Journal of Structural Geology*, *162*, 104679. https://doi.org/10.1016/j.jsg.2022.104679

Kopperud, V., & Myhrvold, T. (2023). *Master's Thesis*. NTNU.

Lunne, T., Long, M., & Uzielli, M. (2006, November). Characterisation and engineering properties of Troll clay. *2nd International Workshop on Characterisation and Engineering Properties of Natural Soils*.

Mulrooney, M. J., Osmond, J. L., Skurtveit, E., Faleide, J. I., & Braathen, A. (2020). Structural analysis of the Smeaheia fault block, a potential CO2 storage site, northern Horda Platform, North Sea. *Marine and Petroleum Geology*, *121*. https://doi.org/10.1016/j.marpetgeo.2020.104598

Nordgård Bolås, H. M., Hermanrud, C., & Teige, G. M. G. (2004). Origin of overpressures in shales: Constraints from basin modeling. *American Association of Petroleum Geologists Bulletin*, *88*(2), 193–211. https://doi.org/10.1306/10060302042

Nygård, R., Gutierrez, M., Gautam, R., & Høeg, K. (2004). Compaction behavior of argillaceous sediments as function of diagenesis. *Marine and Petroleum Geology*, *21*(3), 349–362. https://doi.org/10.1016/j.marpetgeo.2004.01.002

Obradors-Prats, J., Rouainia, M., Aplin, A. C., & Crook, A. J. L. (2019). A Diagenesis Model for Geomechanical Simulations: Formulation and Implications for Pore Pressure and Development of Geological Structures. *Journal of Geophysical Research: Solid Earth*, *124*(5), 4452–4472. https://doi.org/10.1029/2018JB016673

Peric, D., & Crook, A. J. L. (2004). Computational strategies for predictive geology with reference to salt tectonics. *Computer Methods in Applied Mechanics and Engineering*, *193*(48–51), 5195–5222.

Rahman, M. J., Fawad, M., Jahren, J., & Mondol, N. H. (2022). Influence of Depositional and Diagenetic Processes on Caprock Properties of CO2 Storage Sites in the Northern North Sea, Offshore Norway. *Geosciences (Switzerland)*, *12*(5). https://doi.org/10.3390/geosciences12050181

Roberts, D. T., Crook, A. J. L., Cartwright, J. A., Profit, M. L., & Rance, J. M. (2014). The evolution of polygonal fault systems: Insights from geomechanical forward modeling. *48th US Rock Mechanics / Geomechanics Symposium 2014*, *1*(May 2016), 488–502.

Schneider, F., Potdevin, J. L., Wolf, S., & Faille, I. (1996). Mechanical and chemical compaction model for sedimentary basin simulators. *Tectonophysics*, *263*(1–4), 307–317. https://doi.org/10.1016/S0040-1951(96)00027-3

SHARP WP1.1b Report. (2022). *Stress Drivers and Outline of Proposed Numerical Modelling Campaign*.

SHARP WP1.2 Report. (2023). *Lithology Assessment & Constitutive Model* .

SHARP WP3.2 Report. (2023). *Stress and burial history impact on present day state*.

Soldal, M., Skurtveit, E., & Choi, J. C. (2021). Laboratory evaluation of mechanical properties of draupne shale relevant for CO2 seal integrity. *Geosciences (Switzerland)*, *11*(6). https://doi.org/10.3390/geosciences11060244

Thompson, N., Andrews, J. S., Reitan, H., & Teixeira Rodrigues, N. E. (2022, April 27). Data Mining of In-Situ Stress Database Towards Development of Regional and Global Stress Trends and Pore Pressure Relationships. *Day 1 Wed, April 27, 2022*. https://doi.org/10.2118/209525-MS

Thompson, N., Andrews, J. S., Wu, L., & Meneguolo, R. (2022). Characterization of the in-situ stress on the Horda platform – A study from the Northern Lights Eos well. *International Journal of Greenhouse Gas Control*, *114*, 103580. https://doi.org/10.1016/j.ijggc.2022.103580

Thornton, D. A., & Crook, A. J. L. (2014). Predictive Modeling of the Evolution of Fault Structure: 3-D Modeling and Coupled Geomechanical/Flow Simulation. *Rock Mechanics and Rock Engineering*.

Wangen, M., Souche, A., & Johansen, H. (2016). A model for underpressure development in a glacial valley, an example from Adventdalen, Svalbard. *Basin Research*, *28*(6), 752–769. https://doi.org/10.1111/bre.12130

Wensaas, L., Aagaard, P., Berre, T., & Roaldset, E. (1998). Mechanical properties of North Sea Tertiary mudrocks " investigations by triaxial testing of side-wall cores. *Clay Minerals*, *33*, 171–183.

Worden, R. H., Charpentier, D., Fisher, Q. J., & Aplin, A. C. (2005). Fabric development and the smectite to illite transition in Upper Cretaceous mudstones from the North Sea: an image Analysis Approach. *Understanding the Micro to Macro Behaviour of Rock-Fluid Systems, Geological Soceity of London Special Publications*, *249*, 103–114. https://www.lyellcollection.org

Wu, L., Thorsen, R., Ottesen, S., Meneguolo, R., Hartvedt, K., Ringrose, P., & Nazarian, B. (2021). Significance of fault seal in assessing co2 storage capacity and containment risks – an example from the horda platform, northern north sea. *Petroleum Geoscience*, *27*(3). https://doi.org/10.1144/petgeo2020-102

Zadeh, M. K., Mondol, N. H., & Jahren, J. (2017). Velocity anisotropy of upper jurassic organic-rich shales, Norwegian continental shelf. *Geophysics*, *82*(2), C61–C75. https://doi.org/10.1190/geo2016-0035.1